HHS Public Access

Author manuscript

Cell Rep. Author manuscript; available in PMC 2023 October 01.

Published in final edited form as:

Cell Rep. 2023 August 29; 42(8): 112957. doi:10.1016/j.celrep.2023.112957.

Tle4 controls both developmental acquisition and early post-natal maturation of corticothalamic projection neuron identity

Maria J. Galazo[1,3], **David A. Sweetser**[2], **Jeffrey D. Macklis**[1,4,*]

[1]Department of Stem Cell and Regenerative Biology, and Center for Brain Science, Harvard University, Cambridge, MA 02138, USA

[2]Department of Pediatrics, Divisions of Pediatric Hematology/Oncology and Medical Genetics, Massachusetts General Hospital, Boston, MA 02114, USA

[3]Present address: Department of Cell and Molecular Biology, Tulane Brain Institute, Tulane University, New Orleans, LA 70118, USA

[4]Lead contact

SUMMARY

Identities of distinct neuron subtypes are specified during embryonic development, then maintained during post-natal maturation. In cerebral cortex, mechanisms controlling early acquisition of neuron-subtype identities have become increasingly understood. However, mechanisms controlling neuron-subtype identity stability during post-natal maturation are largely unexplored. We identify that *Tle4* is required for both early acquisition and post-natal stability of corticothalamic neuron-subtype identity. Embryonically, *Tle4* promotes acquisition of corticothalamic identity and blocks emergence of core characteristics of subcerebral/corticospinal projection neuron identity, including gene expression and connectivity. During the first post-natal week, when corticothalamic innervation is ongoing, *Tle4* is required to stabilize corticothalamic neuron identity, limiting interference from differentiation programs of developmentally related neuron classes. We identify a deacetylation-based epigenetic mechanism by which TLE4 controls *Fezf2* expression level by corticothalamic neurons. This contributes to distinction of cortical output subtypes and ensures identity stability for appropriate maturation of corticothalamic neurons.

In brief

*Correspondence: jeffrey_macklis@harvard.edu.

AUTHOR CONTRIBUTIONS

M.J.G. and J.D.M. conceived the project and experiments; D.A.S. generated *Tle4* mouse lines; M.J.G. designed and performed experiments; M.J.G. analyzed the data; M.J.G. and J.D.M. interpreted the data and wrote the manuscript. All authors approved the final manuscript.

DECLARATION OF INTERESTS

The authors declare no competing interests.

SUPPLEMENTAL INFORMATION

Supplemental information can be found online at https://doi.org/10.1016/j.celrep.2023.112957.

INCLUSION AND DIVERSITY

We support inclusive, diverse, and equitable conduct of research.

Corticothalamic neurons and subcerebral projection neurons are distinct neuron subtypes that constitute the output of the cerebral cortex. Galazo et al. show that Tle4 promotes acquisition of corticothalamic identity, suppresses subcerebral projection neuron identity in early-born corticofugal neurons during embryonic development, and stabilizes corticothalamic identity during early post-natal maturation.

Graphical abstract

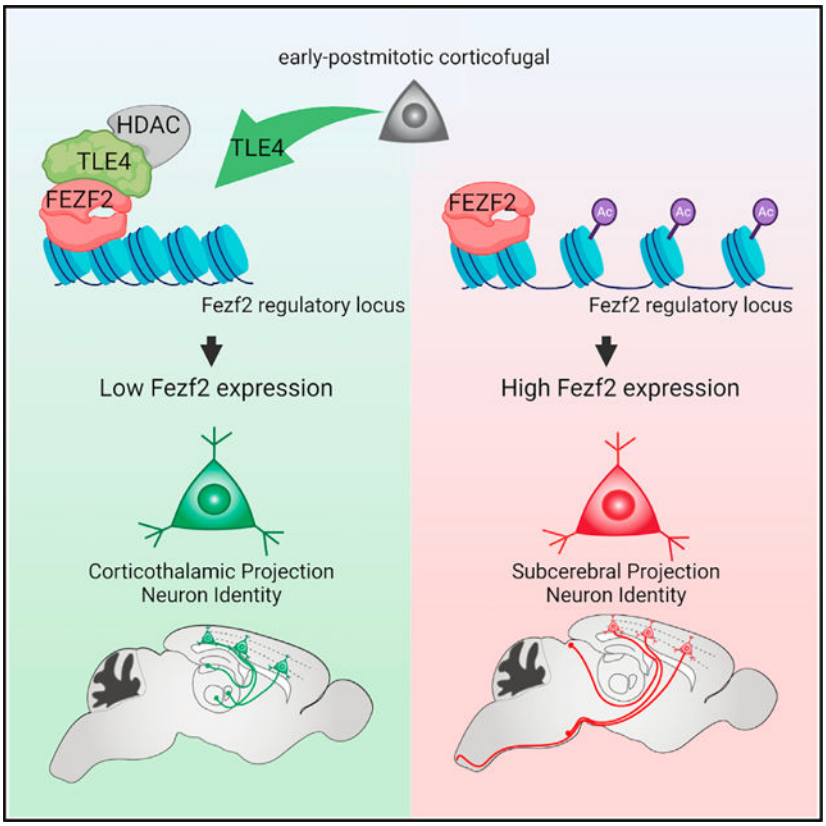

INTRODUCTION

During embryonic development, genetic programs regulate acquisition and progressive refinement of distinct characteristics that constitute neuron identities, including gene expression, afferent and efferent connectivity, electrophysiological properties, molecular signaling, etc.[1–3] In cerebral cortex, neuron-subtype identity has been identified to be controlled both at the progenitor stage and post-mitotically soon after terminal division,[4,5] although multiple studies report that aspects of identity remain malleable through at least early postmitotic development.[6] After initial differentiation, identity appears actively maintained to preserve neuron-subtype characteristics.[7] In cortical neurons, aspects of identity can be altered post-natally by genetic manipulation[8,9] or cortical input activity changes.[10] Some core features of neuron-subtype identity, including gene expression and electrophysiological properties, have been reprogrammed in embryonic and post-natal cortical neurons, resulting in adoption of features of other neuron subtypes.[8,9] This raises

important questions about how neuron subtypes maintain identities in the dynamic context of developing and mature cortex.

Maintenance of neuronal subtype identity is important beyond early development of the nervous system. Failure of neuron identity maintenance is implicated in later neurodegenerative and psychiatric disorders.[7,11] Investigating how distinct cortical neurons acquire, stabilize, and maintain identities during post-natal maturation is critical to understanding cortical development and dysgenesis and to revealing intrinsic vulnerabilities of specific neurons to disorders. Understanding mechanisms controlling identity acquisition and stability *in vivo* could be instrumental to improving *in vitro* differentiation of clinically relevant neuron subtypes for disease modeling. Manipulation of identity stability might provide regulation of cellular plasticity toward neuronal subtype regeneration, repopulation, and/or functional reconstitution in settings of neuronal circuit damage.

Here, we investigate function of *Tle4* in neuron-subtype-specific identity acquisition and stability by corticothalamic projection neurons (CThPN) during murine cortical development and early post-natal maturation. CThPN belong to the broader class of corticofugal projection neurons, including CThPN and subcerebral projection neurons (SCPN). CThPN are born early during corticogenesis, at embryonic day (E) 11.5 to E12.5 in mice, most reside in cortical layer VI (LVI), and they project to thalamus. SCPN are born during mid-corticogenesis (peak at E13.5), reside in layer V (LV), and project to the brainstem and spinal cord.

Tle4 is a non-DNA-binding transcriptional co-repressor important for differentiation in multiple cell types.[12–14] In developing cortex, *Tle4* is frequently used as a corticothalamic marker,[15] and recently, it is identified as a regulator of CThPN development.[16] Previously, we identified *Tle4* as a “CThPN identity gene” because it is highly and specifically expressed by CThPN, both during embryonic development and throughout early post-natal differentiation.[3] Because of its specific and temporally extended expression by CThPN, we hypothesized that *Tle4* might function combinatorially with other regulators of corticofugal and CThPN differentiation to regulate acquisition and stability of CThPN identity during development, circuit formation, and early post-natal maturation.

Our work identifies that *Tle4* is necessary for both acquisition of CThPN identity during embryonic corticogenesis and stability of CThPN identity during early post-natal circuit maturation in the first post-natal week. Without *Tle4*, CThPN do not develop normal molecular, morphological, or projection identity, and instead they acquire hallmark characteristics of SCPN. Importantly, *Tle4* is also necessary during early post-natal maturation to maintain stable CThPN identity. Loss of *Tle4* function during the first postnatal week, when CThPN are establishing connections and circuitry is maturing, results in upregulation of genes characteristic of SCPN, with extension of aberrant axonal projections to subcerebral targets. We identify a deacetylation-based epigenetic mechanism mediated by TLE4 regulating *Fezf2* expression level during acquisition and early post-natal maturation of CThPN identity. This mechanism first blocks emergence of SCPN identity during CThPN specification, then stabilizes distinct identity of CThPN during

circuit establishment and maturation. Thus, *Tle4* actively limits plasticity between these developmentally related classes of cortical projection neurons.

RESULTS

Tle4 is expressed by developing and mature CThPN

Tle4 is expressed in the embryonic cortex and post-natally in LVI,[14,17] where it is specifically expressed by CThPN.[3,15,16] *Tle4* specificity to LVI-CThPN has been determined during early post-natal development. However, whether *Tle4* neuron-subtype-specific expression varies over time and to what extent *Tle4* is expressed by distinct subsets of CThPN have not been investigated.

Using *in situ* hybridization (ISH), we find that *Tle4* is first expressed in the cortical plate at E12.5 by the earliest-born cortical neurons (developing CThPN) (Figure 1B). Expression by progenitors is not detected. Embryonically, *Tle4* is strongly expressed in the subplate and deep cortical plate, where developing CThPN are located (Figure 1C). In previous work comparing gene-expression profiles of cortical projection neurons at embryonic and early post-natal stages,[3] we already determined that *Tle4*-expressing cells in the cortical plate at E18 and LVI at post-natal day (P) 3 and P6 are CThPN (Figure 1A).

During the first post-natal week, most *Tle4*-expressing neurons reside in LVI and subplate, whereas fewer reside in LV (Figures 1C and 1D). *Tle4* expression in LV increases during post-natal development and persists in adults (Figures 1D–1F, cf. P3, P28, and adult). *Tle4* is also expressed in other structures, including claustrum, striatum, and hippocampus. *Tle4* remains highly expressed in LVI and remnants of subplate throughout post-natal maturation and adulthood.

To determine the subtype identity of TLE4$^+$ neurons in LVI, subplate, and LV, we retrogradely labeled three major projection neuron subtypes−CThPN, SCPN, and callosal projection neurons (CPN)−and immunolabeled for TLE4. We confirmed that essentially all LVI-CThPN and CThPN in subplate (SP-CThPN) identified by retrograde labeling from the thalamus with cholera toxin-b (Ctb$^+$) or Fast blue (FB$^+$) and by co-labeling with an LVI-CThPN reporter (*Ntsr1-Cre;tdTomato^{fl}*[18]) express TLE4 (Figures 1H–1K). We confirmed that most TLE4$^+$ neurons in LVI are CThPN (95% CThPN/LVI-TLE4$^+$); however, only 17% of TLE4$^+$ neurons in subplate are CThPN (Figure 1I). Most TLE4$^+$ subplate neurons are Ntsr1-Cre$^-$ (7.5% Ntsr1-Cre$^+$/SP-TLE4$^+$; Figure 1K), consistent with low Ntsr1-Cre expression in subplate vs. high expression in LVI.[19–21] Relatively few CThPN reside in LV.[22,23] LV-CThPN are functionally different from LVI-CThPN. LVI-CThPN constitute most CThPN and project to all thalamic first-order and higher-order nuclei, where they modulate thalamic neurons and do not project to brainstem.[24] In contrast, LV-CThPN project to the thalamus via collateral branches of main axons, which project to brainstem and spinal cord.[22,25] In thalamus, LV-CThPN innervate exclusively high-order thalamic nuclei, where they provide driver inputs to thalamic relay neurons.[26]

To investigate whether LV-TLE4$^+$ neurons are CThPN, we performed dual-retrograde labeling from thalamus (FB injected in somatosensory nuclei) and pyramidal tract (Ctb).

We find that 62% of TLE4$^+$ neurons in LV have dual projections to thalamus and brainstem (FB$^+$-Ctb$^+$) (Figure 1L–1N). This likely under-represents the true number of TLE4$^+$ neurons that are LV-CThPN, because dual-retrograde labeling usually captures a subtotal fraction of a targeted population. Only 2.5% of TLE4$^+$ neurons in LV are SCPN without projection to thalamus (Ctb$^+$-FB$^-$; Figure 1N). We find only very few TLE4$^+$ CPN (Figure 1Q). These data reveal that *Tle4* is constitutively expressed in cortex, that most CThPN (including LV-CThPN and LVI-CThPN) express TLE4, and that most TLE4$^+$ neurons in LV and LVI are CThPN, but not in subplate.

Tle4 promotes differentiation of CThPN identity and prevents acquisition of SCPN identity in early-born cortical neurons

Tle4 is a corepressor with important functions in development of multiple tissues.[12–14] Recently, involvement of *Tle4* in CThPN differentiation was reported using a mutant mouse allele with a *LacZ-ires-Plap* cassette in the fourth intron of *Tle4*.[16] To further investigate functions of *Tle4* in cortical development and CThPN differentiation, we employed a constitutive *Tle4* null mouse mutant allele (termed *Tle4^{KO}*), which disrupts *Tle4* transcription after exon 1 and produces no functional TLE4 protein.[13]

We investigated cortical cytoarchitecture in *Tle4^{KO}* mice at P8. There is no difference in cortical thickness or cytoarchitecture of superficial layers between wild-type (WT) control and *Tle4^{KO}* cortices. However, *Tle4^{KO}* LV is significantly expanded at the expense of LVI (Figures 2A–2D). We refer to this deeper extension of LV as "extended LV" (V_{ex}). LVI is significantly reduced with abnormal cytoarchitecture in which the limits between its upper and lower half, as well as between LVI and subplate, are not clearly discernable by Nissl stain (Figures 2A and 2B). These changes were observed in all areas analyzed, including motor and sensory areas. Further, there is a striking increase in the number of large pyramidal neurons (>20-μm diameter) in LVI and LV_{ex} in the *Tle4^{KO}* cortex, normally only abundant in LV (18% in LVI of WT vs. 42% in LVI–LV_{ex} of *Tle4^{KO}*; $p < 0.01$; Figure 2E). This aberrant presence of large-diameter neurons in LVI is not due to incomplete migration of LV neurons at P8, because it persists in adult *Tle4^{KO}* (Figures S1A and S1B). This LVI reduction with LV expansion in *Tle4^{KO}* hypothetically might be a result of abnormal production, migration, and/or differentiation of neurons. To distinguish between these possibilities, we performed bromodeoxyuridine (BrdU) birth-dating at E11.5, E12.5, E13.5, and E14.5 (peaks of subplate, CThPN, SCPN, and superficial layer-CPN generation, respectively) and analyzed the number and distribution of BrdU$^+$ neurons across layers at P6. There is no significant difference in number or distribution of BrdU$^+$ neurons at these stages (Figure S1C), indicating that neuronal generation and migration are unaffected in *Tle4^{KO}*. These results are consistent with the report of normal neuron migration in *Tle4^{Laz}* mutants.[16]

Because neuron generation and migration are normal in *Tle4^{KO}* cortices, the presence of large-diameter pyramidal neurons in LVI indicates that early-born neurons, which normally become smaller pyramidal LVI-CThPN, do not differentiate normally without *Tle4* and acquire at least a cardinal size of SCPN. Thus, we investigated whether additional

characteristics of SCPN identity emerge in early-born neurons positioned in LVI in the *Tle4*^{KO} cortex.

Long apical dendrites with tufts reaching LII–III and LI are characteristic of SCPN, whereas CThPN usually have shorter apical dendrites extending only to LIV. Using the CThPN-specific reporter *Ntsr1-Cre:tdTomato*^{fl}, we visualized dendrites of neurons that normally become CThPN in the somatosensory cortex of *Tle4*^{KO} and *Tle4*$^{+/-}$ mice. In controls, dendritic apical tufts from *Ntsr1-Cre:tdTomato*$^{+}$ neurons do not extend beyond IV. However, in *Tle4*^{KO}, there are significantly increased tdTomato^{+} apical dendrites aberrantly extending into superficial LII/III and reaching LI (Figures S1E–S1K).

We investigated whether CThPN molecular identity is altered in *Tle4*^{KO}. Using ISH and immunolabeling, we investigated expression of genes known to be expressed by CThPN in LVI and subplate.[3] Across cortical areas, there is a strong downregulation of corticothalamic markers *Fog2*, FOXP2, DARPP32, and *Shb* in LVI and subplate of *Tle4*^{KO} mice (Figures 2F and 2G). Also, there is moderate downregulation of TBR1 and *Cxxc5* in LVI and subplate (Figures S1L–S1M). We investigated potential changes in molecular identity in subplate by analyzing expression of subplate markers *Ctgf* and NURR1[27]; both are also strongly downregulated in the *Tle4*^{KO} cortex.

Consistent with expression reported in *Tle4*^{Laz} mutant mice, we find strong upregulation of SCPN genes (*Fezf2*, CTIP2, *Clim1*, *Crymu*, *Bhlhb5*, *Id2*, *Pcp4*, *S100a10*) by aberrant LVI and subplate neurons in the *Tle4*^{KO} cortex (Figures 2H, 2I, S1N, and S1O). Importantly, there is especially strong upregulation across LVI and subplate of *Fezf2* (SCPN “selector” gene) (Figures 2H and 2I). Together, these results indicate that early-born neurons in LVI and subplate do not develop appropriate CThPN molecular identity or morphology in the *Tle4*^{KO} cortex and instead acquire central SCPN identity characteristics, suggesting either improper identity refinement between these subtypes or a fate switch between them.

To investigate whether abnormally developing CThPN in *Tle4*^{KO} mutants switch fate to become SCPN, we examined whether they extend subcerebral axonal projections. We labeled SCPN by injecting Ctb into the pyramidal tract at P3 and determined their location in cortex at P6. In controls, Ctb^{+} SCPN are restricted to LV. In *Tle4*^{KO} mice, we find significantly more Ctb^{+} SCPN; these are located in LV, LVI, and subplate. Many of the additional Ctb^{+} SCPN are located just deep to the normal LV border, in LV$_{ex}$, appearing as a thicker LV extending deeper into LVI (Figures 3A–3D). We observed this increased distribution of SCPN in all cortical areas analyzed (frontal, parietal, and occipital cortices). Combining BrdU birth-dating and SCPN retrograde labeling, we find significantly more SCPN (Ctb^{+}) born during the usual peak of CThPN neurogenesis in the *Tle4*^{KO} cortex (BrdU at E11.5, $p < 0.01$; BrdU at E12.5, $p < 0.05$; Figures 3K–3M). In the *Tle4*^{KO} cortex, the percentage born at E12.5 that strongly express CTIP2 is increased (Figures 3K–3N), and the percentage born at E11.5–E12.5 that express FOG2 is decreased (Figures 3O–3Q). These results indicate that, in *Tle4*^{KO}mice, many early-born neurons fate-switch to become SCPN.

Early-born neurons might still develop thalamic projections despite abnormal CThPN molecular identity. To investigate this hypothesis, we visualized CThPN axons in

somatosensory thalamic nuclei ventrobasal (VB) and posterior (Po) at P6 using *Ntsr1-Cre:tdTomato*^{fl} (CThPN-specific) and *Emx1-Cre:tdTomato*^{fl} (cortex-specific) reporters crossed into *Tle4*^{KO}. Corticothalamic axons start innervation of somatosensory nuclei at E18.5; by P4, CThPN projections extensively cover these nuclei.[28,29] We find strong reduction of thalamic projections to somatosensory nuclei (VB + Po) in *Ntsr1-Cre:tdTomato*^{fl}*:Tle4*^{KO} (45% reduction, $p < 0.01$; Figure 3G) and *Emx1-Cre:tdTomato*^{fl}*:Tle4*^{KO} mice (30% reduction, $p < 0.05$; Figure 3J) compared with their respective controls.

To investigate whether this reduction in LVI-CThPN projections affects first-order nucleus VB, higher-order nucleus Po, or both, we quantified tdTomato^{+} LVI-CThPN projections in VB and Po independently. We find that LVI-CThPN innervation significantly decreases in both VB and Po (57% reduction in the VB and 40% reduction in Po, relative to innervation in control mice) (Figure 3G). Although thalamic projections are reduced, CThPN still innervate thalamus in mutants, and innervation appears normal, with no aberrant projections to targets outside thalamus, and consistent with the temporal pattern expected at P6.

We investigated whether LVI fate-converted SCPN also bear projections to the thalamus, which would reflect their original corticothalamic fate. We performed dual-retrograde labeling from thalamus and brainstem in mutants and controls. In both *Tle4*^{KO} and controls, there are neurons with dual projections only in LV (normal LV-CThPN population). In *Tle4*^{KO} mice, fate-converted SCPN in LV$_{ex}$ and VI are labeled only from injections in the pyramidal tract, indicating that they do not bear collaterals to thalamus, and thus that they override initial corticothalamic projection identity (Figures 3R–3X). Together, these results demonstrate that in the *Tle4*^{KO} cortex, early-born neurons do not acquire normal CThPN identity, and although many still project to thalamus, others fate-switch and acquire morphological, molecular, and projection identity typical of SCPN.

Fezf2, *Ctip2*, and *Fog2* are dysregulated in all fate-converted SCPN in *Tle4*^{KO} mice

In *Tle4*^{KO} mice, only a subset becomes SCPN (fate-converted SCPN). To investigate molecular changes specifically associated with this switch of projection identity, we identified fate-converted SCPN by retrograde labeling from brainstem, and we analyzed expression of genes critical for axonal projection identity in SCPN (*Fezf2*, *Ctip2*, and *Bhlbh5*)[30–34] and CThPN (*Tbr1*, *Fog2*).[3,35–37]

Fezf2 is critical for SCPN development.[30–32] In *Tle4*^{KO} mice, *Fezf2* is strongly upregulated by virtually all fate-converted SCPN (99% of Ctb^{+} in LV$_{ex}$, 95% of Ctb^{+} LVI and subplate) and also by LVI neurons that do not become SCPN (Figures 4A, 4B, and 4K). This suggests that, although *Fezf2* upregulation is required to convert early-born neurons into SCPN, it is not the only factor responsible for the projection pattern change. Virtually all fate-converted SCPN strongly express CTIP2 (97% of LV$_{ex}$ SCPN, 96% of LVI-subplate SCPN; Figures 4C, 4D, and 4K). In contrast, *Bhlhb5* is specifically expressed by fate-converted SCPN in LV$_{ex}$, but not by fate-converted SCPN in LVI (93% in V$_{ex}$ SCPN, <1% in LVI-subplate SCPN; Figures 4E, 4F, and 4K). *Bhlhb5* is critical for differentiation of specific SCPN subsets.[34] Differential expression of SCPN genes in distinct fate-converted SCPN subsets suggests differences in projection pattern or plasticity.

TBR1 normally determines CThPN identity and represses *Fezf2* in early-born neurons.[35,37] In *Tle4*^{KO} mice, TBR1 expression is slightly reduced but remains in LVI and subplate neurons, where it is co-expressed with *Fezf2*. TBR1 is not expressed by fate-converted SCPN in LV_{ex} but is expressed by fate-converted SCPN in LVI (Figures 4G, 4H, and 4K). This indicates that the level of TBR1 repression of *Fezf2* is context dependent, and that TBR1 expression does not necessarily preclude axonal projection to subcerebral targets.

Importantly, FOG2 is strongly downregulated in *Tle4*^{KO} mice and is barely expressed by any fate-converted SCPN (0% FOG^+-Ctb^+ in V_{ex}, 3% FOG^+-Ctb^+ in LVI-subplate; Figures 4I– 4K). FOG2 downregulates *Ctip2* expression in a context-specific manner and reduces axonal projections to brainstem when mis-expressed in SCPN.[3] Collectively, these data reveal that expressions of *Fezf2*, *Ctip2*, and *Fog2* are dysregulated by all fate-converted SCPN in *Tle4*^{KO} mice, and that fate-converted SCPN in LV_{ex} are more similar to the normal WT SCPN population than to fate-converted SCPN in LVI.

Area-specific projection identity is preserved in the absence of *Tle4*

Although fate-converted SCPN project into the pyramidal tract, it remained possible that they might not reach area-appropriate targets in brainstem and spinal cord corresponding to their cortical area of origin and project instead to inappropriate targets. To investigate this possibility, first, we investigated whether ectopic subcerebral projections exist in *Tle4*^{KO} brains. Because all SCPN, including fate-converted SCPN, strongly express *Fezf2*, we used *Fezf2*$^{+/PLAP}$ mice as a reporter[31] to label SCPN projections in brainstem. In P21 *Fezf2*$^{+/PLAP}$*:Tle4*$^{+/-}$ mice, PLAP-positive axons appropriately innervate superior colliculus and extend along the pyramidal tract. In *Fezf2*$^{+/PLAP}$*:Tle4*^{KO} mice, there are more PLAP-positive axons in superior colliculus (Figures S2A′, S2B′, S3A′, and S3B′), cerebral peduncle, and pyramidal tract (Figures S2A″, S2B″, S2C, S2D, S3A″, and S3B″), but no ectopic projections to abnormal targets (Figures S2A–S2D, S3A, and S3B). The same is true using *Emx1-Cre:tdTomato*^{fl} reporter to label all axons from cortical projection neurons, regardless of their expression of *Fezf2*. There are more $tdTomato^+$ axons in the cerebral peduncle and superior colliculus in *Emx1-Cre:tdTomato*^{fl}*: Tle4*^{KO} compared with controls, but no frankly ectopic projections (Figures S3C–S3H), indicating that fate-converted SCPN do not project aberrantly to inappropriate targets.

We investigated whether fate-converted SCPN project with the same area specificity as normal SCPN. In adult WT mice, SCPN in somatosensory cortex project to pons and superior colliculus, whereas SCPN in visual cortex project only to the superior colliculus.[1,2] Using double labeling from the pyramidal tract at the level of pons (Ctb) and superior colliculus (FB), we investigated whether fate-converted SCPN preserve appropriate area-specific projection targeting (Figure S4A). As expected in adult controls, there are SCPN in LV of somatosensory cortex double-labeled from pons and superior colliculus (Ctb^+-FB^+) (Figures S4B and S4D–S4D″′), and SCPN in LV of visual cortex are labeled from only superior colliculus (FB^+) (Figures S4B and S4F–S4F″′). In *Tle4*^{KO} mice, similarly, there are Ctb^+-FB^+ SCPN in the somatosensory cortex, but they are present more broadly in LV, LV_{ex}, and LVI (Figures S4B and S4E–S4E″′). Importantly, in the *Tle4*^{KO} visual cortex, there are only FB^+ SCPN, again located more broadly in LV, LV_{ex}, and LVI (Figures

S4B and S4G–S4G″′), indicating that fate-converted SCPN remain area appropriate. In the visual cortex, SCPN project specifically to their corresponding visual targets, but not to pons, as do SCPN from other areas (Figure S4C). We investigated area specificity further and confirmed area specificity of *Tle4*^{KO} fate-converted SCPN projections to the spinal cord. Although there are more corticospinal neurons innervating the cervical spinal cord (CSNc) in *Tle4*^{KO} compared with control mice, in both groups, the CSNc is restricted to the rostral motor cortex (Figures S4H–S4J). Therefore, although *Tle4* is critical for distinction of CThPN and SCPN subtype identities, it is not necessary for acquisition of area-specific identity. Fate-converted SCPN resulting from loss of *Tle4* function acquire area-appropriate and area-specific axonal connectivity matching that of endogenous SCPN.

Tle4 is necessary to preserve CThPN identity during circuit formation and maturation

Because *Tle4* is expressed by CThPN from development through adulthood (Figure 1F), we investigated whether *Tle4* might also function during early post-natal CThPN maturation using *Tle4*^{floxed} mice (*Tle4*$^{fl/fl}$).[13] We focused on somatosensory CThPN and induced recombination of the *Tle4*$^{fl/fl}$ allele at two maturation stages: (1) when CThPN axons begin to innervate somatosensory thalamic nuclei (perinatally) and (2) when CThPN are forming synaptic connections with thalamic neurons (during the first postnatal week). In mice, corticothalamic axons start innervating somatosensory nuclei, specifically VB, at E18.5,[28,29,38] and by P′–1 they are establishing immature yet functional synapses that elicit EPSPs in VB neurons.[39,40] By P4, corticothalamic axons have completely covered and innervated somatosensory nuclei VB and Po, as well as other lateral nuclei except for lateral geniculate nucleus (LGN), innervated last.[28]

We investigated the function of *Tle4* when CThPN axons are innervating the thalamus using *Ntsr1-Cre:Tle4*$^{fl/fl}$ mice. First, we determined when *Cre* expression starts in *Ntsr1-Cre* mice and its specificity to CThPN at perinatal stages. Robust *Cre* expression starts at E18 to P′ in the somatosensory cortex in *Ntsr1-Cre;tdTomato*^{fx} mice (Figures S5A–S5D). Therefore, in the *Ntsr1-Cre:Tle4*$^{fl/fl}$ somatosensory cortex, *Tle4* mutation occurs starting at E18, when CThPN axons are invading somatosensory nuclei. We confirmed that *Ntsr1-Cre* is expressed specifically by CThPN at perinatal stages, as well as at post-natal and adult stages. At P1, *Ntsr1-Cre:tdTomato*$^{+}$ neurons express CThPN marker FOG2, but they do not express high-level CTIP2 (Figures S5E and S5F″).

In *Ntsr1-Cre:Tle4*$^{fl/fl}$ mice, *Fezf2* and CTIP2 are upregulated by CThPN, as in *Tle4*^{KO} mice (Figures 5A–5D′). To investigate whether CThPN convert into SCPN, we retrogradely labeled SCPN at P3 and determined their location in the somatosensory cortex at P7. In *Ntsr1-Cre:Tle4*$^{fl/fl}$ mice, in addition to normal LV SCPN, there are retrogradely labeled SCPN in LV_{ex}, LVI, and subplate (Figures 5I, 5I′, and 5J), although these are less abundant than in *Tle4*^{KO} mice. In *Tle4*$^{fl/fl}$ controls, SCPN are restricted appropriately to LV (Figures 5G, 5G′, and 5J). In *Ntsr1-Cre:Tle4*$^{fl/fl}$ mice, LV_{ex} SCPN and LVI SCPN upregulate CTIP2 and downregulate FOG2 expression, as in *Tle4*^{KO} mice (Figures 5K and 5L). This indicates that both molecular and projection identity can be “reprogrammed” in CThPN at stages when their axons have already started to innervate the thalamus (E18 to P0).

To investigate whether axonal projections of reprogrammed SCPN (LV_{ex} SCPN and LV SCPN) are transitory or stable, we visualized axons of *Ntsr1-Cre*$^{+}$ neurons in the pyramidal tract of *Ntsr1-Cre:tdTomato*^{fl}:*Tle4*$^{fl/fl}$ and *Ntsr1-Cre:tdTomato*^{fl}*: Tle4*$^{fl/WT}$ control mice at P28. As expected, there are no tdTomato^{+} axons in the pyramidal tract of *Ntsr1-Cre:tdTomato*^{fl}*: Tle4*$^{fl/WT}$ controls (Figures 5M, 5M′, and 5O). Strikingly, there are tdTomato^{+} axons in the pyramidal tract of *Ntsr1-Cre: tdTomato*^{fl}:*Tle4*$^{fl/fl}$ mice (Figures 5N, 5N′, and 5O), indicating that reprogrammed SCPN maintain durable projections to subcerebral targets.

We investigated whether reprogramming of CThPN into SCPN by loss of *Tle4* function can be induced even later, after corticothalamic synapses have already become functional. In somatosensory nuclei, corticothalamic synapses elicit EPSPs by P1.[39] We injected adeno-associated virus (AAV)-encoding Cre (AAV-Cre) at P3 in one cortical hemisphere and control-AAV virus in the contralateral cortex of *tdTomato*^{fl}:*Tle4*$^{fl/fl}$ mice (Figure 6A). We confirmed that recombination starts 24–48 h after AAV-Cre injection. Remarkably, *Fezf2* is still upregulated in LVI and subplate in the AAV-Cre-injected area, but not in control contralateral cortex (Figures 6B and 6B′). Also, other SCPN molecular controls are upregulated and CThPN molecular controls are downregulated in LVI in the AAV-Cre injected area, but not in the contralateral cortex (Figure S6). These results indicate that loss of *Tle4* function between P3 and P5 reprograms molecular identity of CThPN.

To investigate whether projection identity is also plastic and might be reprogrammed at this post-natal maturation stage, we performed AAV-Cre and control-AAV injections at P3, retrogradely labeled SCPN at P5, and determined their location in cortex at P12. Quite strikingly, there are non-standard, retrogradely labeled SCPN in LVI and subplate (reprogrammed from CThPN) in the AAV-Cre-injected area, but not in the control contralateral area (Figures 6C and 6D). These reprogrammed SCPN are located at a range of depths in LVI and subplate (Figure 6D), but we do not identify a distinct LV_{ex} as in *Ntsr1-Cre:tdTomato*^{fl}:*Tle4*$^{fl/fl}$ or *Tle4*^{KO} mice.

Together, these data indicate that *Tle4* expression is necessary to preserve molecular and projection identity of CThPN during circuit formation and early post-natal maturation, and that some CThPN can reprogram both their molecular and projection identity at stages when corticothalamic synapses already have been established and the circuit is maturing.

TLE4 and FEZF2 form a transcription-regulatory complex that modulates activation of *Fezf2*-regulatory regions in developing CThPN

Distinct levels of *Fezf2* are required for correct development of distinct corticofugal subtypes: high *Fezf2* expression by SCPN and low *Fezf2* expression by CThPN.[30–32,41] In *Tle4*^{KO} mice, abnormally high expression of *Fezf2* by CThPN likely disrupts their differentiation. TLE4 and FEZF2 proteins interact directly,[16,42] and importantly both regulate CThPN development.[16] However, how TLE4 and FEZF2 proteins function together in regulating CThPN differentiation has not been addressed. We hypothesized that a TLE4-FEZF2 complex regulates *Fezf2* expression by developing CThPN to achieve correct *Fezf2* dosage required for appropriate CThPN differentiation and distinction from SCPN.

To investigate this hypothesis, we first confirmed that TLE4 and FEZF2 interact in cortical neurons at E15.5 via co-immunoprecipitation (coIP) of TLE4-FLAG and HA-FEZF2 proteins (Figure 7A). FEZF2 contains an Engrailed1 (Eh1) homology domain, which binds to either the C-terminal tryptophan-aspartic repeat (WDR) domain (also called WD40) or the N-terminal Q-domain of TLE co-repressors.[43–46] To determine the specific domain of TLE4 required for interaction with FEZF2, we generated truncated forms of TLE4 lacking either the WDR domain (FLAG-TLE4-ΔWDR) or the Q-oligomerization domain (FLAG-TLE4-ΔQ), and we tested their ability to pull down HA-FEZF2. CoIP experiments reveal that, although full-length FLAG-TLE4 and FLAG-TLE4-ΔQ bind and pull down HA-FEZF2, FLAG-TLE4-ΔWDR does not pull down HA-FEZF2 (Figure 7A). These results indicate that the WDR domain is required for interaction of TLE4 with FEZF2.

Next, we investigated whether TLE4 and FEZF2 bind to putative regulatory regions flanking the *Fezf2* locus. Two putative regulatory regions (3 kb upstream and 4.5 kb downstream of *Fezf2*) were selected for analysis based on their sequence conservation in mammals, presence of defined enhancers, and presence of predicted FEZF2-binding motifs.[47,48] To investigate whether TLE4 and FEZF2 bind to loci in these putative *Fezf2* regulatory regions, we performed chromatin immunoprecipitation (ChIP) from E15.5 neurons expressing HA-FEZF2 and FLAG-TLE4, followed by qPCR with overlapping primer sets to fully screen the *Fezf2*-downstream region (loci 1–23; Figure 7B). Compared with non-specific IgG pull-down, ChIP with anti-HA antibody (ChIP-FEZF2) was enriched in loci in both *Fezf2*-upstream and -downstream regions. However, ChIP with anti-FLAG antibody (ChIP-TLE4) was enriched only in loci downstream of *Fezf2*. Therefore, we focused on the region 4.5 kb downstream of *Fezf2* as a putative regulatory region controlled by TLE4-FEZF2.

Loci with >10-fold enrichment by ChIP-FEZF2 and ChIP-TLE4 were considered co-occupied by FEZF2-TLE4. Under this strict selection criterion, we identify two loci co-occupied by FEZF2-TLE4 in the *Fezf2*-downstream region (locus [LC] 7: ChIP-FEZF2 51-fold, ChIP-TLE4 29-fold; LC17: ChIP-FEZF2 10-fold, ChIP-TLE4 153-fold; Figure 7B).

The presence of two neighboring co-occupied loci suggests that the *Fezf2*-downstream region is regulated by the FEZF2-TLE4 complex. However, to directly investigate this possibility, we tested transcriptional activity from this region under multiple conditions. We cloned this putative regulatory region into a luciferase reporter construct (pGL3-*Fezf2*-downstream-luc) and transfected E15.5 WT neurons with either pGL3-*Fezf2*-downstream-luc alone (baseline control) or together with constructs to express TLE4, FEZF2, or TLE4+FEZF2 (Figure 7D). Relative to baseline activation (*Fezf2*-downstream-luc), either TLE4 or FEZF2 reduces transcriptional activation from this region (28% luc-activity reduction with TLE4, 42% reduction with FEZF2; Figure 7D). Strikingly, when both TLE4 and FEZF2 are co-transfected, reduction is stronger (60% luc-activity reduction). Together with results identifying loci co-occupied by TLE4 and FEZF2 (Figure 7B), these data strongly suggest that the FEZF2-TLE4 complex regulates transcription in the *Fezf2*-downstream region.

However, it was theoretically possible that co-expressed TLE4 and FEZF2 might bind to other factors instead of working together to downregulate transcription. To investigate the

requirement of the FEZF2-TLE4 complex for regulation in the *Fezf2*-downstream region, we investigated the activity of pGL3-*Fezf2*-downstream-luc in the presence of a truncated form of FEZF2 (FEZF2-ZF), which preserves the zinc-finger DNA-binding domain but lacks the Eh1 domain that binds TLE4. FEZF2-ZF strongly activates transcription from the *Fezf2*-downstream region (Figure 7D), supporting the interpretation that FEZF2 interaction with TLE4 (or with other co-repressors via the Eh1 domain) is necessary to downregulate expression from this region.

To investigate the requirement of TLE4 for regulation in the *Fezf2*-downstream region, we tested the activity of pGL3-*Fezf2*-downstream-luc in cortical neurons from E15.5 *Tle4*^{KO} embryos. The cortical plate at E15.5 is mostly composed of developing deep-layer neurons, which in *Tle4*^{KO} embryos strongly express *Fezf2*. Transcription from the *Fezf2*-downstream region is strongly downregulated after expression of TLE4 alone or TLE4+FEZF2 in *Tle4*^{KO} neurons (81% lucactivity reduction with TLE4, 62% luc-activity reduction with TLE4+FEZF2; Figure 7E), indicating that the presence of TLE4 is critical for strong repression in this region. Importantly, expression of non-functional forms of TLE4 (TLE4-DWDR or TLE4-DQ) does not alter transcriptional activity (Figure 7E). Interestingly, expression of FEZF2 alone in *Tle4*^{KO} neurons downregulates activity of pGL3-*Fezf2*-downstream-luc (49% luc-activity reduction with FEZF2; Figure 7E), suggesting that FEZF2 might recruit other co-repressors, in addition to TLE4, to regulate activity in this region. Further, we investigated the requirement of FEZF2 for regulation of the *Fezf2*-downstream region using neurons from E15.5 *Fezf2*^{KO} embryos (Figure 7F). In *Fezf2*^{KO} mice, expression of TLE4 by cortical neurons is reduced.[16,31] After rescuing expression of FEZF2 in *Fezf2*^{KO} neurons, activity of pGL3-*Fezf2*-downstream-luc is downregulated (33% luc-activity reduction with FEZF2), and it is strongly downregulated after co-expression of TLE4+FEZF2 (60% luc-activity reduction with TLE4+FEZF2; Figure 7F). Importantly, transfection of TLE4 alone in *Fezf2*^{KO} neurons does not affect activity of pGL3-*Fezf2*-downstream-luc, indicating that FEZF2 is required for recruitment of TLE4 as a co-repressor to regulate transcription in the *Fezf2*-downstream region. Collectively, these data indicate that TLE4 and FEZF2 form a regulatory complex that downregulates transcriptional activity from the *Fezf2*-downstream region, and although FEZF2 conceivably might also recruit other factors, TLE4-mediated repression in this region depends on the presence of FEZF2.

TLE4-FEZF2 complex modulates chromatin state of loci regulating *Fezf2* expression during CThPN differentiation and maturation

TLE4 binds histone deacetylases (HDACs) to mediate repression.[49,50] HDACs recruited to loci co-occupied by FEZF2-TLE4 in the *Fezf2*-downstream region might likely change chromatin conformation state at these loci, compacting chromatin and reducing *Fezf2* expression level. We investigated whether the acetylation level at co-occupied locicorrelates with level ofexpression of *Fezf2* by distinct corticofugal subtypes and with expression of *Fezf2* by CThPN at progressive developmental stages.

Because *Fezf2* is strongly expressed by SCPN and *Tle4*^{KO}-CThPN and is weakly expressed by WT CThPN, we compared acetylation level at LC7, co-occupied by TLE4-FEZF2 (Figure 7B) in these three neuron populations. We isolated WT SCPN,

CThPN, and *Tle4*^{KO}-CThPN from *Rbp4-Cre:tdTomato*^{fl}, *Ntsr1-Cre: tdTomato*^{fl}, and *Ntsr1-Cre:tdTomato*^{fl}*:Tle4*$^{fl/fl}$ P0 pups, respectively, and performed ChIP-qPCR for the open chromatin mark acetylated histone 3-lysine 9 (AcHis3K9). ChIP-AcHis3K9 qPCR values at LC7 were normalized to ChIP-AcHis3K9 qPCR values at a constitutively active locus (*Gapdh*). In WT CThPN, LC7 is significantly less acetylated than in SCPN (5-fold enrichment in WT-CThPN vs. 18-fold enrichment in SCPN; $p < 0.01$; Figure 7C). This is consistent with the presence of FEZF2-TLE4 complex recruiting HDACs to this locus in CThPN, but not in SCPN, in which lack of TLE4 expression prevents formation of the complex. Importantly, LC7 is also significantly more acetylated in *Tle4*^{KO}-CThPN than in WT-CThPN (5-fold enrichment in WT-CThPN vs. 9.6-fold enrichment in *Tle4*^{KO}-CThPN; $p < 0.05$; Figure 7C). In comparison, acetylation level at a locus of the *Fezf2*-downstream region not co-occupied by TLE4 and FEZF2 (LC13) is not significantly different between WT-CThPN, SCPN, and *Tle4*^{KO}-CThPN (0.5-fold enrichment in SCPN, 0.3-fold enrichment in WT-CThPN, 0.22-fold enrichment in *Tle4*^{KO}-CThPN; Figure 7C). Therefore, we identify at least one locus (LC7) co-occupied by FEZF2-TLE4 differentially acetylated in CThPN, SCPN, and *Tle4*^{KO}-CThPN and that reduced acetylation at this locus correlates with lower *Fezf2* expression in these corticofugal neuron subtypes.

We investigated whether the acetylation level at LC7 changes during CThPN embryonic and post-natal differentiation, reflecting *Fezf2* expression changes by CThPN during this period. Embryonic CThPN express *Fezf2* strongly, but *Fezf2* is progressively reduced post-natally and maintained at a low level (Figure 7G). We isolated E15.5 cortical neurons, P0 CThPN, and P6 CThPN (from P0 and P6 *Ntsr1-Cre:tdTomato*^{fl} mice) and performed ChIP-AcHis3K9 qPCR at LC7. Strikingly, acetylation at LC7 drastically decreases post-natally compared with E15.5 (152-fold enrichment at E15.5, 58-fold enrichment at P0, 13.8-fold enrichment at P6; $p < 0.01$; Figure 7H). Importantly, the acetylation level of a nearby locus not co-occupied by FEZF2-TLE4 (LC13) does not change overtime(Figure 7H). Therefore, progressive deacetylation at loci regulated by FEZF2-TLE4 complex correlates with progressive reduction of *Fezf2* expression by CThPN during differentiation.

DISCUSSION

Our results reveal that *Tle4* is necessary during embryonic development for acquisition of precise CThPN identity by early-born cortical neurons and for differentiated CThPN to preserve distinct identity during early post-natal maturation. We identify mechanistically that TLE4 is recruited by FEZF2 to control the expression level of *Fezf2* in CThPN during embryonic and post-natal development. This epigenetic mechanism contributes importantly to distinction of corticofugal subtypes and ensures appropriate maturation of CThPN.

Consistent with observations in *Tle4*$^{LacZ/LacZ}$ mice,[16] our experiments reveal substantial abnormalities of CThPN development in *Tle4*^{KO} mice.[13] In both *Tle4* mutant models, the expression of important SCPN controls are upregulated by CThPN, expression of CThPN controls are downregulated, dendritic development of CThPN is abnormal, and projection to thalamus appears along the normal trajectory, although reduced in *Tle4*^{KO} mice, indicating that *Tle4* is necessary to acquire CThPN identity but does not directly instruct CThPN axons to extend into the thalamus. In *Tle4*^{KO} mice, specific subsets of neurons fate-switch

and become SCPN. These neurons not only exhibit abnormal gene expression but also abnormal SCPN-like somatic morphology, with axonal projections to the brainstem and/or spinal cord. Although some phenotypic differences between mutant models are expected because of differing gene-targeting approaches, overall, results of loss of *Tle4* function across both mutant models largely overlap, revealing the importance of *Tle4* function in CThPN development.

Without *Tle4*, strong upregulation of *Fezf2* by developing CThPN contributes importantly to their abnormal differentiation. *Fezf2* is critical for differentiation of corticofugal neurons and to instruct SCPN identity.[30–32] Elegant experiments by Tsyporin et al.[16] highlighted the importance of *Fezf2* in regulating CThPN development and suggested that FEZF2 and TLE4 together regulate CThPN differentiation. Our work mechanistically identifies that the FEZF2-TLE4 complex controls CThPN differentiation by regulating the level of expression of *Fezf2* by CThPN. TLE4 is recruited by FEZF2 to control chromatin conformation at loci regulating *Fezf2* expression during CThPN embryonic and post-natal development. This epigenetic mechanism contributes to critical regulation of FEZF2 dosage for appropriate distinction of corticofugal subtypes embryonically and for postnatal maturation of CThPN.

Our data support the emerging interpretation that intrinsic molecular diversity of CThPN contributes to their differential plasticity, rendering some specific CThPN subsets more amenable to fate-switch into SCPN.[3,51] The result that fate-converted SCPN in LV_{ex} are more similar to normal WT SCPN than fate-converted SCPN in LVI is consistent with the idea that distinct CThPN subsets have intrinsic expression differences that contribute to their differential plasticity. These intrinsic differences might be critical for correct implementation of the SCPN identity program following upregulation of *Fezf2.*

Tle4 functions are important beyond corticofugal differentiation, potentially enabling control over directed differentiation or *trans*-differentiation of corticofugal lineages. There is substantial interest in understanding how to differentiate specific neuron subtypes *in vitro* that faithfully reflect the characteristics of neuron subtypes *in vivo*[6,52] and in reprogramming existing neuron types into others to replace or compensate for those selectively vulnerable in disease, e.g., SCPN in amyotrophic lateral sclerosis (ALS)/motor neuron disease (MND). For such hypothetical approaches to offer optimal benefit, conversion to, e.g., SCPN, would need to reflect broad connectivity and molecular features of desired new neuron subtypes, not just a few molecular markers. Regulation by *Tle4* loss of function of broad SCPN molecular expression and connectivity offers promise in this regard.

Some aspects of neuron-subtype identity remain plastic at least briefly after initial development. Characteristics of cortical neuron identity, including gene expression, dendritic morphology, and electrophysiological properties, have been reprogrammed early post-natally in mice.[8,9] However, projection identity of cortical projection neurons has been successfully reprogrammed only embryonically. Mis-expression of *Fezf2* in CPN at E17.5 induces extension of axonal projections to subcortical structures.[8] However, it is important to note that, at this stage, CPN are immature and are still extending axons dorsal to striatum toward the midline, amenable to re-direction ventrally into the striatum. Re-direction

of SCPN connectivity by cortical neurons has not been previously reported at later developmental or post-natal stages.

Our experiments inducing *Tle4* mutation post-natally reveal a more extended time window for neuron plasticity and projection identity reprogramming in CThPN compared with other cortical neuron subtypes. It is striking that some CThPN can change their axonal connectivity even after P3, especially because they are the earliest-born cortical neuron subtype, and they are establishing synaptic connections in the thalamus at this post-natal stage. It will be interesting to understand whether this extended time window for identity reprogramming exhibited by CThPN reflects intrinsically enhanced capacity for plasticity of this subtype, or perhaps reflects that identity reprogramming might be more effectively accomplished between neuron subtypes with similar developmental trajectories (in this case between corticofugal subtypes).

The epigenetic mechanism identified here contributes to establishing distinction between CThPN and SCPN subtypes and to maintaining CThPN identity during post-natal maturation. Developing CThPN express TLE4 as soon as they are positioned in the cortical plate. The TLE4-FEZF2 complex likely starts functioning at this early stage to progressively reduce FEZF2 expression level and thus direct correct acquisition of CThPN identity. Post-natally, continuous *Tle4* expression and function of the TLE4-FEZF2 complex in CThPN ensure low-level expression of *Fezf2*, which our experiments identify as necessary to maintain CThPN identity and avoid reprogramming into SCPN. Similarly, *Tbr1* is critical for development of CThPN identity by early-born cortical neurons, and its continued expression is important for maintaining CThPN molecular identity, dendritic morphology, and synaptic properties.[11] Together, *Tle4* and *Tbr1* might regulate complementary mechanisms controlling maintenance of broad molecular and input-output connectivity characteristics of CThPN identity. Interestingly, other important developmental controls over cortical neuron-subtype identity, including *Fezf2*,[30–32] *Ctip2*,[33] *Sox5*,[53,54] *Couptf1*,[51] and *Fog2*,[3] are also expressed continuously during post-natal cortical development (Allen Mouse Brain Atlas: http://mouse.brain-map.org). Perhaps they might also have additional functions during neuron maturation that are not yet investigated. Our work here underscores the importance of regulating not only early neuron identity acquisition but also neuron-subtype identity stability during maturation for correct long-term functions of neurons.

Limitations of the study

In *Tle4*^{KO} mice, there might be additional, perhaps subtle, alterations of CThPN, such as intra-thalamic rearrangement of projections. Changes in patterns of LV-CThPN and LVI-CThPN projections to first-order and higher-order nuclei are one conceivable possibility. This kind of cross-hierarchical intrathalamic plasticity has been observed in sensory nuclei after sensory deprivation.[55–57] In our experiments, we find no change in number of LV-CThPN in *Tle4*^{KO}, but our experiments did not investigate whether subtle intra-thalamic projection phenotypes or intra-thalamic plasticity occurs, so we cannot exclude this possibility.

STAR★METHODS

RESOURCE AVAILABILITY

Lead contact—Further information and requests for resources and reagents should be directed to and will be fulfilled by the lead contact, Dr. Jeffrey D. Macklis (jeffrey_macklis@harvard.edu), or via AddGene for already-deposited constructs.

Materials availability—All unique/stable reagents generated in this study are available with a materials transfer agreement from the lead contact for academic, non-commercial use; negotiation and completion of a materials transfer agreement with Harvard University is required if there is potential for commercial application.

Data and code availability

- The DOIs of key resources are listed in the key resource table. Other data reported on this paper will be shared by the lead contact upon request.
- This paper does not report original code.
- Any additional information required to reanalyze the data reported in this paper is available from the lead contact upon request.

EXPERIMENTAL MODEL AND STUDY PARTICIPANT DETAILS

All mouse studies were approved by the Harvard University or previously Massachusetts General Hospital IACUCs, and were performed in accordance with institutional and federal guidelines. *Tle4*^{KO} and *Tle4*^{floxed} mice were described in.[13] *Emx1*-Cre (stock number 005628) and tdTomato^{fl} (Ai14-*Rosa26-tdTomato*$^{fl\text{-}stop\text{-}fl}$; stock number 007914) mice were purchased from Jackson Laboratories. *Ntsr1*-Cre (RRID:MGI_3836636, stock number 030648-UCD) and *Rbp4*-Cre ((RRID:MGI_4367067, stock number 031125-UCD) mice were generated by the GENSAT project,[59] and were purchased from MMRRC. *Fezf2-PLAP* mice were the generous gift of Dr. S. McConnell at Stanford University.[31] The morning of vaginal plug detection was designated D′.5, and the day of birth as P0. Unless noted otherwise, all experiments with *Tle4*^{KO} were controlled with *Tle4*$^{+/+}$, although no abnormal cortical phenotypes were observed in *Tle4*$^{+/-}$.

METHOD DETAILS

Immunocytochemistry and *in situ* hybridization—Brains were fixed and stained using standard methods.[30,53] Primary antibodies and dilutions used: rat anti-BrdU, 1:750 (Accurate Chemical and Scientific Corporation Cat# OBT-0030 RRID:AB_2341179); rat anti-CTIP2, 1:500 (Abcam Cat# ab28448, RRI-D:AB_1140055); rabbit anti-DARPP-32, 1:250 (Cell Signaling Technology Cat# 2306S, RRID:AB_823479); rabbit anti-FOG2, 1:250 (Santa Cruz Cat# sc-10755, RRID:AB_2218978); goat anti-NURR1, 1:100 (R&D Systems Cat# AF2156, RRID:AB_2153894); rabbit anti-TBR1, 1:500 (Abcam Cat# ab31940, RRID:AB_2200219); rabbit anti-FOXP2 1:1000 (Abcam Cat# ab1307, RRID:AB_1268914); rabbit anti-TLE4, 1:200 (Santa Cruz Biotechnology Cat# sc-9125, RRID:AB_793141). Rat anti-BrdU requires antigen retrieval, as described in.[60] ISH was performed as previously described in.[33] cDNA clones for riboprobes are listed in.[3]

Retrograde labeling—Projection neurons were retrograde labeled from their axon terminals by pressure injection of Alexa-conjugated cholera toxin B (Ctb, Invitrogen) or Fast Blue (Polysciences) at distinct stages. In postnatal pups, injections into either the cerebral peduncle, pyramidal tract, cervical spinal cord, dorsal thalamus, or cortex were performed under ultrasound backscatter microscopy guidance (Vevo 770, VisualSonics, Toronto) at P3 or P5, depending on the experimental condition. In adults, stereotaxic injections into the superior colliculus or pyramidal tract-pontine nuclei were performed following coordinates from[61] Paxinos and Franklin, *The Mouse Brain in Stereotaxic Coordinates, 2nd edition*, 2001. The number of mice and genotypes for each experiment are specified in each figure legend.

BrdU birthdating—Timed pregnant females were injected with bromodeoxyuridine (50 mg/kg, i.p) at E11.5, E12.5, E13.5, or E14.5. For experiments in which BrdU birthdating was combined with SCPN retrograde labeling, Ctb-Alexa555 was injected into the cerebral peduncle at P3. Brains were collected at P6, and processed for either 1) BrdU and CTIP2 or 2) BrdU and FOG2 dual immunocytochemistry. Co-localization and quantification of SCPN, $BrdU^+$, and $CTIP2^+$ or $FOG2^+$ neurons, and their distribution within cortical layers was analyzed using established methods.[30,53,62] Number of mice and genotypes for each experiment are specified in each figure legend.

Viral injections—Viral injections were performed under ultrasound backscatter microscopy guidance (Vevo 770, VisualSonics, Toronto) at P3. *TdTomato^{fl}:Tle4$^{fl/fl}$* mice were injected with 70 μL of AAV-Cre, distributed in several injection sites in one hemisphere of the cortex, and 70 μL of AAV-control in the contralateral hemisphere. AAV-Cre or AAV-control serotype 2.1 were obtained from the Massachusetts General Hospital Viral Core. Number of mice and genotypes for each experiment are specified in each figure legend.

Protein Co-Immunoprecipitation—Dissociated E15.5 cortical neurons were co-transfected with *HA-Fezf2* and either *Flag-Tle4*, *Flag-TLE4ΔQ, or Flag-TLE4ΔWDR* constructs, using Amaxa nucleofection (Lonza). Protein IP was performed using Protein-A/G agarose beads (Pierce), following standard methods.[3,63] Mouse anti-Flag and non-specific mouse IgG (4 mg/ml; Sigma F7425; RRIB:AB_439687) were used for pull-down. Rabbit anti-HA (1:2000, Covance, MMS-101R, RRID:AB_291262) was used for immunoblotting. Number of mice and genotypes for each experiment are specified in each figure legend.

ChIP-qPCR—For ChIP-FEZF2 and ChIP-TLE4, dissociated E15.5 cortical neurons were co-transfected with *HA-Fezf2* and *Flag-Tle4* constructs, using Amaxa nucleofection (Lonza). ChIP-qPCR was performed following standard methods. In brief, double crosslinking (protein-protein, and protein-DNA) was performed using EGS cross-linker (ethylene glycol bis-sulfosuccinimidyl succinate) or formaldehyde, respectively, according to.[64] Chromatin shearing was optimized for the amplicon size. Anti-Flag (Sigma F7425; RRIB:AB_439687), anti-HA (Covance, MMS-101R, RRID:AB_291262), or non-specific IgG antibodies were used for ChIP bound to protein G/A beads. Pulled-down chromatin

was purified and quantified by qPCR (LightCycler Fast start DNA Master SYBER Green I, Roche) with overlapping sets of primers designed to cover a region approximately 4.5 kb downstream of Fezf2 (chr14: 12,337,560.12,342,460). Amplicon average size is 300 bp. A list of chromosome coordinates for each amplicon is provided in Table S1. For each amplicon, the fold-enrichment listed is of anti-Flag pull-down over IgG or anti-HA pull-down over IgG, using the ΔCt method.

ChIP-AcH3K9 was performed using either wildtype cortical neurons obtained from E15.5 embryos, P0, or P3 pups, or using FACS-purified CThPN, SCPN, or *Tle4*^{KO}-CThPN obtained from *Ntsr1-Cre:tdTomato*^{fl}, *Rbp4-Cre:tdTomato*^{fl}, or *Ntsr1-Cre:tdTomato*^{fl}*: Tle4*^{KO} E15.5 embryos, respectively. FACS purification was performed as described in Arlotta et al., 2005.[33] Anti-AcH3K9 (Millipore 17–658, RRID:AB_1587124) or non-specific IgG antibodies were used for ChIP bound to protein G/A beads. Pulled-down chromatin was quantified by qPCR. Fold-enrichment was determined by normalizing ΔCt values for each locus against IgG control, and against a constitutive active locus (*Gapdh*). For ChIP experiments, n = 4 independent replicates were used per group.

Luciferase assay—The 4.5 kb downstream of *Fezf2* was obtained from a BAC clone (RP23–141E17), and cloned into pGL3-Firefly luciferase upstream of the SV40 promoter (pGL3-luc; Promega) using a Gibson assembly kit (New England BioLabs) to generate pGL3-*Fezf2*-downstramluc. Dissociated neurons from dissected E15.5 wildtype, *Tle4*^{KO}, or *Fezf2*^{KO} cortices were nucleofected with pGL3-*Fezf2*-downstram-luc, Renilla luciferase vector, and either *Tle4, Fezf2, Fezf2-ZF, TLE4ΔQ, or TLE4ΔWDR* expression plasmids, alone or in combination, depending on the experimental condition (n = 7 independent biological replicates per condition for luciferase experiments with neurons from wildtype and *Tle4*^{KO} embryos, and n = 5 replicates per condition for luciferase experiments with neuros from *Fezf2*^{KO} neurons). Luciferase activities were assayed 48 h later using the Dual-Glo system (Promega). Firefly/Renilla luciferase ratio was calculated for each condition and referred to as the percentage relative to the baseline activity of pGL3-*Fezf2*-downstram-luc alone.

Imaging and quantification—Epifluorescence or brightfield images illustrating brain hemisections or large tissue areas were acquired using a Nikon 90i with a tilemontaging imaging function. Images for quantitative analyses were acquired with a Zeiss LSM 780 confocal microscope. Laser power and gain were adjusted until <1% of pixels were saturated. Imaging parameters were identical for all samples within the same experiment.

For cell quantification, z-slices spanning the entire cortical thickness (from pia to white matter) were acquired. Cell counting was performed with FIJI on single z-slices in a rectangular region of interest (ROI) of constant width (500 μm, horizontal dimension) and variable height (adjusted to match the cortical thickness, which varies depending on the age of mice analyzed for each experiment). At least 3 sections per brain were analyzed in one or multiple cortical areas, as indicated in the figure legend for each specific experiment. For quantifications within specific layers, Nissl, Dapi, or ToPro3 counterstains were used for the histological definition of layer boundaries. For cell quantification and cell distribution

calculation across the cortex, the ROIs were divided into 10 bins of equal size across their vertical dimension (bin 1 at the pia, bin 10 at the border with white matter).

For quantification of corticothalamic axon innervation in somatosensory thalamic nuclei, the boundaries of the ventrobasal nuclei (VB) and posterior nuclei (Po) were identified using Dapi counterstain or expression of genes defining the borders of these nuclei (FOG2 labeling defines the exterior border of VB with the reticular nucleus, and FOXP2 defines the border of the Po). ROIs that include the VB, Po, and VB + Po were defined. For quantification of tdTomato$^+$ pixels, 8-bit monochrome images corresponding to the tdTomato signal (representing CThPN axonal projections) were used. TdTomato$^+$ pixels in each ROI were then identified by thresholding in NIH ImageJ. The total area of thresholded TdTomato$^+$ pixels was measured using the “Analyze Particles” function. The percentage of area occupied by TdTomato$^+$ pixels in each ROI (VB, Po, or VB + Po) was calculated.

For quantification of axons innervating the tectum and cerebral peduncle, 8-bit monochrome images corresponding to tdTomato signal (representing SCPN axon projections innervating these structures) were used. Images first had threshold adjustment using the “Feature J” function on ImageJ, such that the intensity on unlabeled parts of the tissue (without a labeled axon) was zero. For measurements within the cerebral peduncle, an ROI for the cerebral peduncle area (Cped area) was identified. The borders of Cped area were identified using Dapi counterstain and expression of Foxp2 (marks the border with the adjacent subthalamic nucleus). TdTomato$^+$ pixels in the Cped area were identified by thresholding in NIH ImageJ. The total area of thresholded TdTomato$^+$ pixels was measured using the “Analyze Particles” function. The percentage of area occupied by TdTomato$^+$ pixels in the Cped area was calculated. For measurements in the tectal areas, we define the border between the thalamus and pretectal area. Intensity of tdTomato pixels along the thalamus-tectum border was quantified using the “Analyze Particles” function on ImageJ.

For quantification of dendritic extension, fluorescence intensity measurements were performed on rectangular ROIs of 250 μm width (horizontal dimension) and height adjusted to match the cortical thickness (vertical dimension). ROIs were split into 10 bins of equal size across their vertical dimension (bin 1 at the pia, bin 10 at the border with white matter). Fluorescence intensity was measured in 8-bit monochrome images corresponding to tdTomato signal (representing CThPN somata, dendrites, and axon projections). Fluorescence intensity in the white matter is constant across samples and was used for normalization of the intensity in the overlying ROI. Then, tdTomato fluorescence intensity was measured in each bin using the ImageJ “Mean Intensity” function and expressed as a percentage of the maximum value in the intensity range value (256).

QUANTIFICATION AND STATISTICAL ANALYSIS

Details of imaging quantification methodologies are described in star method details. All n values and p values obtained are listed in the figure legends. GraphPad Prism version 8 (GraphPad Software, Inc., San Diego, CA) was used to perform statistical tests. Data distributions were assumed to be normal, but this was not formally tested. No statistical methods were used to pre-determine sample sizes.

We used unpaired two-tailed Student's t-tests or one-way ANOVA followed by Tukey post hoc test for statistical comparison. The specific test used for each analysis is indicated in the figure legends. Values are represented as means ± SEM. Statistical significance is noted by asterisks, (*$p < 0.05$, **$p < 0.01$), or otherwise indicated.

Supplementary Material

Refer to Web version on PubMed Central for supplementary material.

ACKNOWLEDGMENTS

We thank E. Gornstein, C. Greppi, I. Florea, and K. Yee for technical assistance; members of the Macklis laboratory for discussions; Harvard Center for Biological Imaging for infrastructure and support; and S.K. McConnell for sharing of *Fezf2-PLAP* mice. This work was supported by grants from the NIH (R01 NS045523, with additional infrastructure support from NS075672, NS049553, NS104055, and DP1 NS106665), Robert and Emily Pearlstein Fund, Jane and Lee Seidman Fund, and Max and Anne Wien Professor of Life Sciences fund (to J.D.M.). M.J.G. was supported by fellowships from CajaMadrid Foundation and Spanish Ministry of Education, Brain and Behavior Foundation, Tulane COR-faculty grant, and Louisiana Board of Regents (LEQSF(2021–24)-RD-A-14). J.D.M. is an Allen Distinguished Investigator of the Paul G. Allen Frontiers Group.

REFERENCES

1. Greig LC, Woodworth MB, Galazo MJ, Padmanabhan H, and Macklis JD (2013). Molecular logic of neocortical projection neuron specification, development and diversity. Nat. Rev. Neurosci. 14, 755–769. 10.1038/nrn3586. [PubMed: 24105342]
2. Lodato S, and Arlotta P. (2015). Generating neuronal diversity in the mammalian cerebral cortex. Annu. Rev. Cell Dev. Biol. 31, 699–720. 10.1146/annurev-cellbio-100814-125353. [PubMed: 26359774]
3. Galazo MJ, Emsley JG, and Macklis JD (2016). Corticothalamic Projection Neuron Development beyond Subtype Specification: Fog2 and Intersectional Controls Regulate Intraclass Neuronal Diversity. Neuron 91, 90–106. 10.1016/j.neuron.2016.05.024. [PubMed: 27321927]
4. Frantz GD, and McConnell SK (1996). Restriction of late cerebral cortical progenitors to an upper-layer fate. Neuron 17, 55–61. 10.1016/s0896-6273(00)80280-9. [PubMed: 8755478]
5. Shen Q, Wang Y, Dimos JT, Fasano CA, Phoenix TN, Lemischka IR, Ivanova NB, Stifani S, Morrisey EE, and Temple S. (2006). The timing of cortical neurogenesis is encoded within lineages of individual progenitor cells. Nat. Neurosci. 9, 743–751. 10.1038/nn1694. [PubMed: 16680166]
6. Rouaux C, Bhai S, and Arlotta P. (2012). Programming and reprogramming neuronal subtypes in the central nervous system. Dev. Neurobiol. 72, 1085–1098. 10.1002/dneu.22018. [PubMed: 22378700]
7. Deneris ES, and Hobert O. (2014). Maintenance of postmitotic neuronal cell identity. Nat. Neurosci. 17, 899–907. 10.1038/nn.3731. [PubMed: 24929660]
8. Rouaux C, and Arlotta P. (2013). Direct lineage reprogramming of postmitotic callosal neurons into corticofugal neurons in vivo. Nat. Cell Biol. 15, 214–221. 10.1038/ncb2660. [PubMed: 23334497]
9. De la Rossa A, Bellone C, Golding B, Vitali I, Moss J, Toni N, Lüscher C, and Jabaudon D. (2013). In vivo reprogramming of circuit connectivity in postmitotic neocortical neurons. Nat. Neurosci. 16, 193–200. 10.1038/nn.3299. [PubMed: 23292682]
10. Chevée M, Robertson JDJ, Cannon GH, Brown SP, and Goff LA (2018). Variation in Activity State, Axonal Projection, and Position Define the Transcriptional Identity of Individual Neocortical Projection Neurons. Cell Rep. 22, 441–455. 10.1016/j.celrep.2017.12.046. [PubMed: 29320739]
11. Fazel Darbandi S, Robinson Schwartz SE, Qi Q, Catta-Preta R, Pai ELL, Mandell JD, Everitt A, Rubin A, Krasnoff RA, Katzman S, et al. (2018). Neonatal Tbr1 Dosage Controls Cortical Layer 6 Connectivity. Neuron 100, 831–845.e7. 10.1016/j.neuron.2018.09.027. [PubMed: 30318412]

12. Xing S, Shao P, Li F, Zhao X, Seo W, Wheat JC, Ramasamy S, Wang J, Li X, Peng W, et al. (2018). Tle corepressors are differentially partitioned to instruct CD8(+) T cell lineage choice and identity. J. Exp. Med. 215, 2211–2226. 10.1084/jem.20171514. [PubMed: 30045946]
13. Wheat JC, Krause DS, Shin TH, Chen X, Wang J, Ding D, Yamin R, and Sweetser DA (2014). The corepressor Tle4 is a novel regulator of murine hematopoiesis and bone development. PLoS One 9, e105557. 10.1371/journal.pone.0105557.
14. Yao J, Liu Y, Husain J, Lo R, Palaparti A, Henderson J, and Stifani S. (1998). Combinatorial expression patterns of individual TLE proteins during cell determination and differentiation suggest non-redundant functions for mammalian homologs of Drosophila Groucho. Dev. Growth Differ. 40, 133–146. 10.1046/j.1440-169x.1998.00003.x. [PubMed: 9572356]
15. Molyneaux BJ, Goff LA, Brettler AC, Chen HH, Hrvatin S, Rinn JL, and Arlotta P. (2015). DeCoN: genome-wide analysis of in vivo transcriptional dynamics during pyramidal neuron fate selection in neocortex. Neuron 85, 275–288. 10.1016/j.neuron.2014.12.024. [PubMed: 25556833]
16. Tsyporin J, Tastad D, Ma X, Nehme A, Finn T, Huebner L, Liu G, Gallardo D, Makhamreh A, Roberts JM, et al. (2021). Transcriptional repression by FEZF2 restricts alternative identities of cortical projection neurons. Cell Rep. 35, 109269. 10.1016/j.celrep.2021.109269. [PubMed: 34161768]
17. Allen T, and Lobe CG (1999). A comparison of Notch, Hes and Grg expression during murine embryonic and post-natal development. Cell. Mol. Biol. 45, 687–708. [PubMed: 10512199]
18. Tasic B, Menon V, Nguyen TN, Kim TK, Jarsky T, Yao Z, Levi B, Gray LT, Sorensen SA, Dolbeare T, et al. (2016). Adult mouse cortical cell taxonomy revealed by single cell transcriptomics. Nat. Neurosci. 19, 335–346. 10.1038/nn.4216. [PubMed: 26727548]
19. Kim J, Matney CJ, Blankenship A, Hestrin S, and Brown SP (2014). Layer 6 corticothalamic neurons activate a cortical output layer, layer 5a. J. Neurosci. 34, 9656–9664. 10.1523/jneurosci.1325-14.2014. [PubMed: 25031405]
20. Zolnik TA, Ledderose J, Toumazou M, Trimbuch T, Oram T, Rosenmund C, Eickholt BJ, Sachdev RNS, and Larkum ME (2020). Layer 6b Is Driven by Intracortical Long-Range Projection Neurons. Cell Rep. 30, 3492–3505.e5. 10.1016/j.celrep.2020.02.044. [PubMed: 32160552]
21. Hoerder-Suabedissen A, Hayashi S, Upton L, Nolan Z, Casas-Torremocha D, Grant E, Viswanathan S, Kanold PO, Clasca F, Kim Y, and Molná r Z. (2018). Subset of Cortical Layer 6b Neurons Selectively Innervates Higher Order Thalamic Nuclei in Mice. Cerebr. Cortex 28, 1882–1897. 10.1093/cercor/bhy036.
22. Veinante P, Lavallé e P, and Deschênes M. (2000). Corticothalamic projections from layer 5 of the vibrissal barrel cortex in the rat. J. Comp. Neurol. 424, 197–204. 10.1002/1096-9861(20000821)424:2<197::aid-cne1>3.0.co;2-6. [PubMed: 10906697]
23. Killackey HP, and Sherman SM (2003). Corticothalamic projections from the rat primary somatosensory cortex. J. Neurosci. 23, 7381–7384. 10.1523/jneurosci.23-19-07381.2003. [PubMed: 12917373]
24. Guillery RW, and Sherman SM (2002). Thalamic relay functions and their role in corticocortical communication: generalizations from the visual system. Neuron 33, 163–175. 10.1016/s0896-6273(01)00582-7. [PubMed: 11804565]
25. Deschênes M, Bourassa J, and Pinault D. (1994). Corticothalamic projections from layer V cells in rat are collaterals of long-range corticofugal axons. Brain Res. 664, 215–219. 10.1016/0006-8993(94)91974-7. [PubMed: 7895031]
26. Sherman SM (2016). Thalamus plays a central role in ongoing cortical functioning. Nat. Neurosci. 19, 533–541. 10.1038/nn.4269. [PubMed: 27021938]
27. Hoerder-Suabedissen A, Wang WZ, Lee S, Davies KE, Goffinet AM, Rakić S, Parnavelas J, Reim K, Nicolić M, Paulsen O, and Molnár Z. (2009). Novel markers reveal subpopulations of subplate neurons in the murine cerebral cortex. Cerebr. Cortex 19, 1738–1750. 10.1093/cercor/bhn195.
28. Jacobs EC, Campagnoni C, Kampf K, Reyes SD, Kalra V, Handley V, Xie YY, Hong-Hu Y, Spreur V, Fisher RS, and Campagnoni AT (2007). Visualization of corticofugal projections during early cortical development in a tau-GFP-transgenic mouse. Eur. J. Neurosci. 25, 17–30. 10.1111/j.1460-9568.2006.05258.x. [PubMed: 17241263]

29. Auladell C, Pérez-Sust P, Supèr H, and Soriano E. (2000). The early development of thalamocortical and corticothalamic projections in the mouse. Anat. Embryol. 201, 169–179. 10.1007/pL0008238.
30. Molyneaux BJ, Arlotta P, Hirata T, Hibi M, and Macklis JD (2005). Fezl is required for the birth and specification of corticospinal motor neurons. Neuron 47, 817–831. 10.1016/j.neuron.2005.08.030. [PubMed: 16157277]
31. Chen B, Schaevitz LR, and McConnell SK (2005). Fezl regulates the differentiation and axon targeting of layer 5 subcortical projection neurons in cerebral cortex. Proc. Natl. Acad. Sci. USA 102, 17184–17189. 10.1073/pnas.0508732102. [PubMed: 16284245]
32. Chen JG, Rasin MR, Kwan KY, and Sestan N. (2005). Zfp312 is required for subcortical axonal projections and dendritic morphology of deep-layer pyramidal neurons of the cerebral cortex. Proc. Natl. Acad. Sci. USA 102, 17792–17797. 10.1073/pnas.0509032102. [PubMed: 16314561]
33. Arlotta P, Molyneaux BJ, Chen J, Inoue J, Kominami R, and Macklis JD (2005). Neuronal subtype-specific genes that control corticospinal motor neuron development in vivo. Neuron 45, 207–221. 10.1016/j.neuron.2004.12.036. [PubMed: 15664173]
34. Joshi PS, Molyneaux BJ, Feng L, Xie X, Macklis JD, and Gan L. (2008). Bhlhb5 regulates the postmitotic acquisition of area identities in layers II-V of the developing neocortex. Neuron 60, 258–272. 10.1016/j.neuron.2008.08.006. [PubMed: 18957218]
35. Hevner RF, Shi L, Justice N, Hsueh Y, Sheng M, Smiga S, Bulfone A, Goffinet AM, Campagnoni AT, and Rubenstein JL (2001). Tbr1 regulates differentiation of the preplate and layer 6. Neuron 29, 353–366. 10.1016/s0896-6273(01)00211-2. [PubMed: 11239428]
36. McKenna WL, Betancourt J, Larkin KA, Abrams B, Guo C, Rubenstein JLR, and Chen B. (2011). Tbr1 and Fezf2 regulate alternate corticofugal neuronal identities during neocortical development. J. Neurosci. 31, 549–564. 10.1523/JNEUROSCI.4131-10.2011. [PubMed: 21228164]
37. Han W, Kwan KY, Shim S, Lam MMS, Shin Y, Xu X, Zhu Y, Li M, and Sestan N. (2011). TBR1 directly represses Fezf2 to control the laminar origin and development of the corticospinal tract. Proc. Natl. Acad. Sci. USA 108, 3041–3046. 10.1073/pnas.1016723108. [PubMed: 21285371]
38. Grant E, Hoerder-Suabedissen A, and Molnár Z. (2012). Development of the corticothalamic projections. Front. Neurosci. 6, 53. 10.3389/fnins.2012.00053. [PubMed: 22586359]
39. Golshani P, Warren RA, and Jones EG (1998). Progression of change in NMDA, non-NMDA, and metabotropic glutamate receptor function at the developing corticothalamic synapse. J. Neurophysiol. 80, 143–154. 10.1152/jn.1998.80.1.143. [PubMed: 9658036]
40. Liu XB, Murray KD, and Jones EG (2004). Switching of NMDA receptor 2A and 2B subunits at thalamic and cortical synapses during early postnatal development. J. Neurosci. 24, 8885–8895. 10.1523/jneurosci.2476-04.2004. [PubMed: 15470155]
41. Lodato S, Molyneaux BJ, Zuccaro E, Goff LA, Chen HH, Yuan W, Meleski A, Takahashi E, Mahony S, Rinn JL, et al. (2014). Gene coregulation by Fezf2 selects neurotransmitter identity and connectivity of corticospinal neurons. Nat. Neurosci. 17, 1046–1054. 10.1038/nn.3757. [PubMed: 24997765]
42. Zhang S, Li J, Lea R, Vleminckx K, and Amaya E. (2014). Fezf2 promotes neuronal differentiation through localised activation of Wnt/b-catenin signalling during forebrain development. Development 141, 4794–4805. 10.1242/dev.115691. [PubMed: 25468942]
43. Buscarlet M, and Stifani S. (2007). The 'Marx' of Groucho on development and disease. Trends Cell Biol. 17, 353–361. 10.1016/j.tcb.2007.07.002. [PubMed: 17643306]
44. Jennings BH, Pickles LM, Wainwright SM, Roe SM, Pearl LH, and Ish-Horowicz D. (2006). Molecular recognition of transcriptional repressor motifs by the WD domain of the Groucho/TLE corepressor. Mol. Cell. 22, 645–655. 10.1016/j.molcel.2006.04.024. [PubMed: 16762837]
45. Chen G, and Courey AJ (2000). Groucho/TLE family proteins and transcriptional repression. Gene 249, 1–16. 10.1016/s0378-1119(00)00161-x. [PubMed: 10831834]
46. Shimizu T, and Hibi M. (2009). Formation and patterning of the forebrain and olfactory system by zinc-finger genes Fezf1 and Fezf2. Dev. Growth Differ. 51, 221–231. 10.1111/j.1440-169X.2009.01088.x. [PubMed: 19222525]

47. Eckler MJ, Larkin KA, McKenna WL, Katzman S, Guo C, Roque R, Visel A, Rubenstein JLR, and Chen B. (2014). Multiple conserved regulatory domains promote Fezf2 expression in the developing cerebral cortex. Neural Dev. 9, 6. 10.1186/1749-8104-9-6. [PubMed: 24618363]
48. Sugimoto M, Fujikawa A, Womack JE, and Sugimoto Y. (2006). Evidence that bovine forebrain embryonic zinc finger-like gene influences immune response associated with mastitis resistance. Proc. Natl. Acad. Sci. USA 103, 6454–6459. 10.1073/pnas.0601015103. [PubMed: 16611727]
49. Bandyopadhyay S, Valdor R, and Macian F. (2014). Tle4 regulates epigenetic silencing of gamma interferon expression during effector T helper cell tolerance. Mol. Cell Biol. 34, 233–245. 10.1128/MCB.00902-13. [PubMed: 24190972]
50. Brantjes H, Roose J, van De Wetering M, and Clevers H. (2001). All Tcf HMG box transcription factors interact with Groucho-related co-repressors. Nucleic Acids Res. 29, 1410–1419. 10.1093/nar/29.7.1410. [PubMed: 11266540]
51. Tomassy GS, De Leonibus E, Jabaudon D, Lodato S, Alfano C, Mele A, Macklis JD, and Studer M. (2010). Area-specific temporal control of corticospinal motor neuron differentiation by COUP-TFI. Proc. Natl. Acad. Sci. USA 107, 3576–3581. 10.1073/pnas.0911792107. [PubMed: 20133588]
52. Barker RA, Götz M, and Parmar M. (2018). New approaches for brain repair-from rescue to reprogramming. Nature 557, 329–334. 10.1038/s41586-018-0087-1. [PubMed: 29769670]
53. Lai T, Jabaudon D, Molyneaux BJ, Azim E, Arlotta P, Menezes JRL, and Macklis JD (2008). SOX5 controls the sequential generation of distinct corticofugal neuron subtypes. Neuron 57, 232–247. 10.1016/j.neuron.2007.12.023. [PubMed: 18215621]
54. Kwan KY, Lam MMS, Krsnik Z, Kawasawa YI, Lefebvre V, and Sestan N. (2008). SOX5 postmitotically regulates migration, postmigratory differentiation, and projections of subplate and deep-layer neocortical neurons. Proc. Natl. Acad. Sci. USA 105, 16021–16026. 10.1073/pnas.0806791105. [PubMed: 18840685]
55. Grant E, Hoerder-Suabedissen A, and Molnár Z. (2016). The Regulation of Corticofugal Fiber Targeting by Retinal Inputs. Cerebr. Cortex 26, 1336–1348. 10.1093/cercor/bhv315.
56. Giasafaki C, Grant E, Hoerder-Suabedissen A, Hayashi S, Lee S, and Molnár Z. (2022). Cross-hierarchical plasticity of corticofugal projections to dLGN after neonatal monocular enucleation. J. Comp. Neurol. 530, 978–997. 10.1002/cne.25304. [PubMed: 35078267]
57. Frangeul L, Pouchelon G, Telley L, Lefort S, Luscher C, and Jabaudon D. (2016). A cross-modal genetic framework for the development and plasticity of sensory pathways. Nature 538, 96–98. 10.1038/nature19770. [PubMed: 27669022]
58. Maguire CA, Bovenberg MS, Crommentuijn MH, Niers JM, Kerami M, Teng J, Sena-Esteves M, Badr CE, and Tannous BA (2013). Triple bioluminescence imaging for in vivo monitoring of cellular processes. Mol. Ther. Nucleic Acids 2, e99. 10.1038/mtna.2013.25. [PubMed: 23778500]
59. Gong S, Doughty M, Harbaugh CR, Cummins A, Hatten ME, Heintz N, and Gerfen CR (2007). Targeting Cre recombinase to specific neuron populations with bacterial artificial chromosome constructs. J. Neurosci. 27, 9817–9823. 10.1523/JNEUROSCI.2707-07.2007. [PubMed: 17855595]
60. Magavi SS, and Macklis JD (2008). Identification of newborn cells by BrdU labeling and immunocytochemistry in vivo. Methods Mol. Biol. 438, 335–343. 10.1007/978-1-59745-133-8_25. [PubMed: 18369768]
61. Paxinos G, and Franklin KBJ (2001). The Mouse Brain in Stereotaxic Coordinates, 2nd edition Edition (Elsevier).
62. Woodworth MB, Greig LC, Liu KX, Ippolito GC, Tucker HO, and Macklis JD (2016). Ctip1 Regulates the Balance between Specification of Distinct Projection Neuron Subtypes in Deep Cortical Layers. Cell Rep. 15, 999–1012. 10.1016/j.celrep.2016.03.064. [PubMed: 27117402]
63. Huggins GS, Bacani CJ, Boltax J, Aikawa R, and Leiden JM (2001). Friend of GATA 2 physically interacts with chicken ovalbumin upstream promoter-TF2 (COUP-TF2) and COUP-TF3 and represses COUP-TF2-dependent activation of the atrial natriuretic factor promoter. J. Biol. Chem. 276, 28029–28036. 10.1074/jbc.M103577200. [PubMed: 11382775]

64. Forster N, Saladi SV, van Bragt M, Sfondouris ME, Jones FE, Li Z, and Ellisen LW (2014). Basal cell signaling by p63 controls luminal progenitor function and lactation via NRG1. Dev. Cell 28, 147–160. 10.1016/j.devcel.2013.11.019. [PubMed: 24412575]

Highlights

- *Tle4* promotes CThPN identity and blocks SCPN identity in early-born cortical neurons
- *Tle4* is necessary to maintain CThPN identity during circuit maturation
- TLE4-FEZF2 complex regulates *Fezf2* expression in developing CThPN
- TLE4-FEZF2 regulates corticofugal subtypes distinction and developmental maturation of CThPN

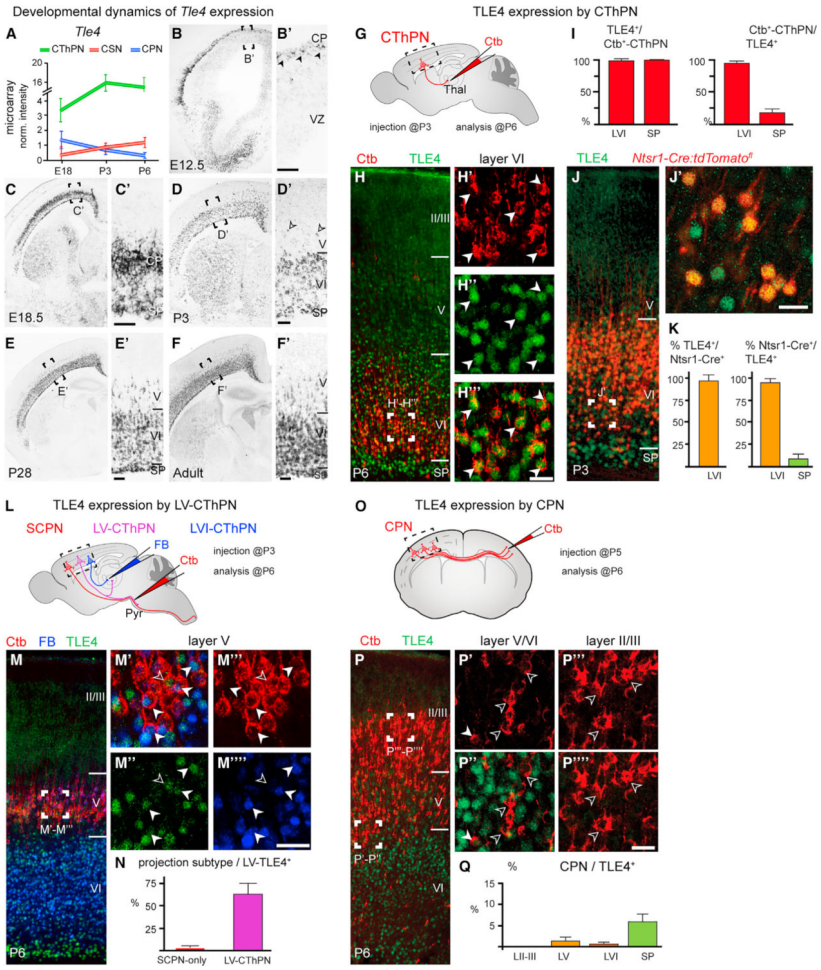

Figure 1. Developmental dynamics and neuron-subtype specificity of *Tle4* expression

(A) *Tle4* expression by CThPN (green), CSN (red), and CPN (blue) at E18, P3, and P6 (adapted from Galazo et al.[3]).

(B–F) *Tle4* ISH at E12.5, E18.5, P3, P28, and adult (n = 4 mice, embryonic ages; n = 3 mice, post-natal ages). (B and B′) *Tle4* is first expressed by neurons in cortical plate (CP) at E12.5 (black arrowheads). At P3, most *Tle4*$^{+}$ neurons are in LVI and few in LV (D′, open arrowheads). At P28, more neurons in LV express *Tle4* (E and E′).

(G, L, and O) Approaches for neuron-subtype identification.

(H) TLE4 immunocytochemistry (green) on P6 brains injected with Ctb (red) in thalamus at P3. Images are from the motor cortex. (H′ and H‴) Confocal images are from box in (H).

(I) Percentages of CThPN expressing TLE4 (98% TLE4^{+}/LVI-CThPN, 99% TLE4^{+}/SP-CThPN) and CThPN/TLE4^{+} cells (95% CThPN/LVI-TLE4^{+}, 17% CThPN/SP-TLE4^{+}). Quantification in somatosensory and motor areas (n = 4).

(J) TLE4 immunolabeling in *Ntsr1-Cre:tdTomato*^{fl} somatosensory cortex at P3 (n = 4). (J′) High-magnification confocal image from box in (J).

(K) Overlap between TLE4 and *Ntsr1-Cre:tdTomato*^{fl} reporter (96% TLE4^{+}/Ntsr1-Cre^{+}, 94% Ntsr1-Cre^{+}/LVI-TLE4^{+}, 7.5% Ntsr1-Cre^{+}/SP-TLE4^{+}).

(L) Approach to identify dual-projecting LV-CThPN. FB (blue) and Ctb (red) were injected in somatosensory thalamus and pyramidal tract, respectively, at P3 (n = 6).

(M–M‴) TLE4 (green) co-localization with FB and Ctb in somatosensory cortex.
(N) 62.2% of LV-TLE4$^+$ neurons are LV-CThPN (FB$^+$-Ctb$^+$/LV-TLE4$^+$, white arrowheads in M′–M‴). 2.5% of LV-TLE4$^+$ neurons are SCPN (Ctb$^+$/LV-TLE4$^+$, open arrowheads in M–M′).
(O–Q) Only rare CPN (Ctb$^+$) express TLE4 (CPN/TLE4$^+$, 0% LII–III, 1.4% LV, 0.4% LVI, 6% SP; TLE4$^+$-Ctb$^+$, solid arrow; TLE4$^-$-Ctb$^+$, open arrows; quantifications in motor and somatosensory areas; n = 4).
Error bars, SEM. Scale bars, 50 μm (B′–F′); 20 μm (H′, J′, M′–M′, and P′–P‴′).

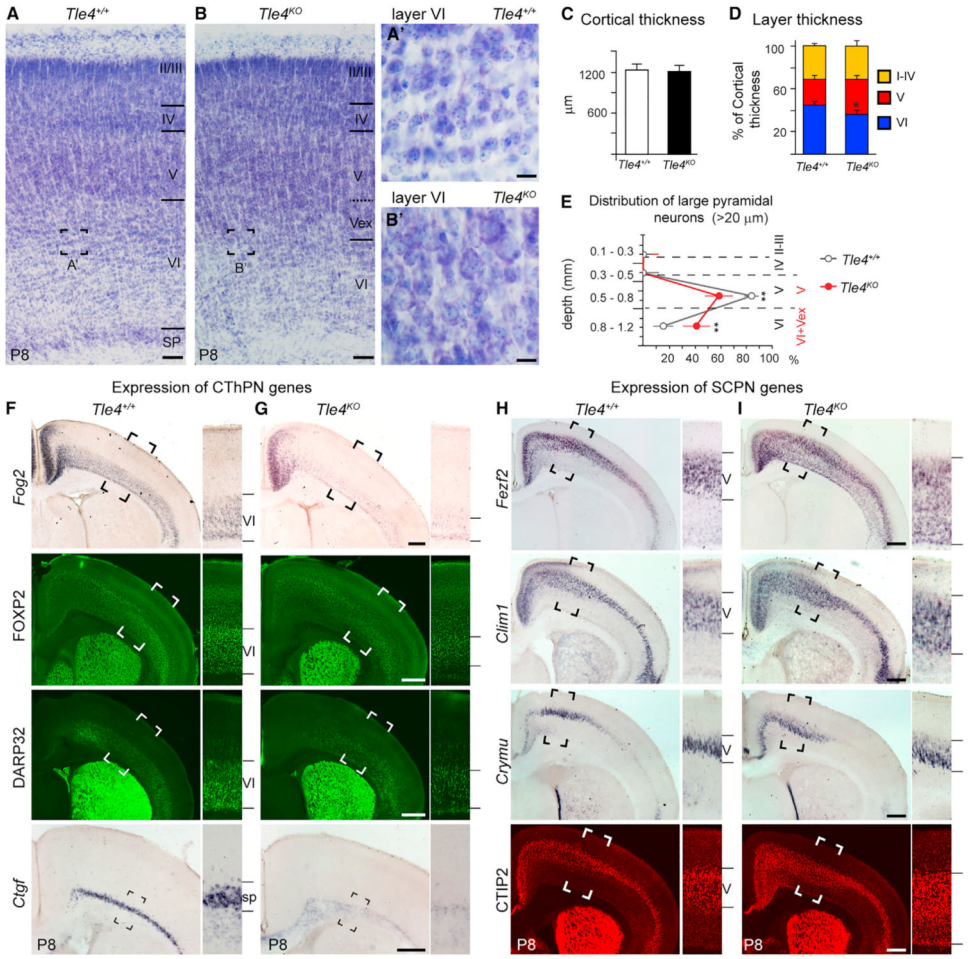

Figure 2. In the absence of *Tle4* function, CThPN do not develop normal identity and acquire somatic morphology and gene expression characteristic of SCPN

(A–D) Nissl staining in WT and *Tle4*^{KO} mice (P8). Images from motor-somatosensory border area. (A′ and B′) Somatic morphology of neurons at depth corresponding to LVI, (C) cortical thickness, and (D) layer thickness in *Tle4*^{KO} and control mice in somatosensory cortex.

(E) Quantification of large pyramidal neurons (diameter >20 µm) across cortical thickness (n = 4 per genotype; unpaired t test, *p < 0.05, **p < 0.01). Mean ± SEM.

(F–I) Decreased expression of CThPN genes (*Fog2*, FOXP2, TBR1, and *Ctgf*) and increased expression of SCPN genes (*Fezf2*, *Clim1*, *Crymu*, CTIP2) in *Tle4*^{KO} mice at P8 (n = 4 per genotype). Insets magnify boxed areas.

Scale bars, 100 µm (A and B); 20 µm (A′ and B′); 500 µm (F–I).

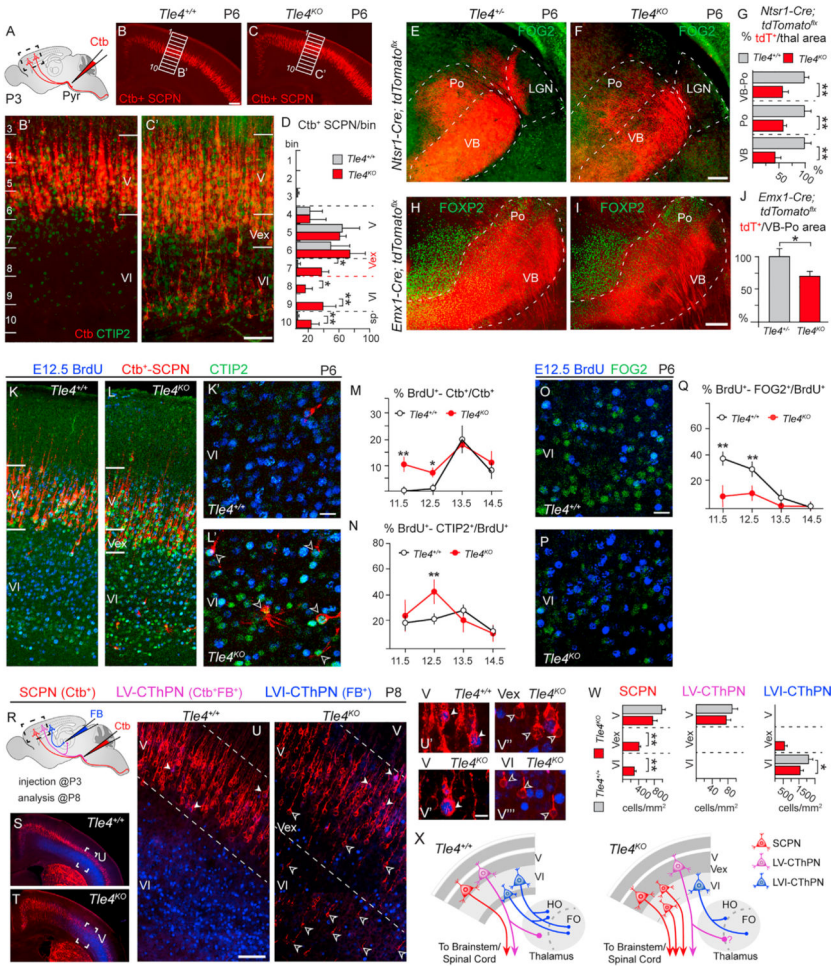

Figure 3. In the *Tle4*^{KO} cortex, more early-born neurons become SCPN and fewer develop as CThPN

(A) SCPN labeling approach via injection of Ctb into the pyramidal tract (pyr) at P3. Analysis at P6.

(B and C) SCPN (Ctb^{+}) across the medio-lateral extent of cortex. (B′ and C′) Insets magnify labeling in the somatosensory cortex (grid in B and C).

(D) Distribution of SCPN across cortical thickness (divided in 10 equal bins). Mean Ctb^{+} cells/bin ± SEM. *p < 0.05, **p < 0.01, n = 6 mice per genotype.

(E–J) Projections to thalamus are reduced in *Tle4*^{KO} mice. CThPN axons (red) labeled via *Ntsr1-Cre:tdTomato*^{fl} (E and F) and *Emx1-Cre:tdTomato*^{fl} reporters (H and I). (G) Percentage of area occupied by TdTomato^{+} pixels in ventrobasal (VB), posterior (Po), and VB + Po nuclei in *Ntsr1-Cre:tdTomato*^{fl}*:Tle4*$^{+/-}$ and *Ntsr1-Cre:tdTomato*^{fl}*:Tle4*^{KO} and in (J) VB + Po nuclei in *Emx1-Cre:tdTomato*^{fl}*:Tle4*$^{+/-}$ and *Emx1-Cre:tdTomato*^{fl}*:Tle4*^{KO} mice at P6 (n = 4 per genotype; unpaired t test, *p < 0.05, **p < 0.01). FOG2 and FOXP2 define the borders of VP-Po.

(K–Q) In the *Tle4*^{KO} cortex, more early-born neurons project as SCPN and express CTIP2 strongly, and fewer express FOG2. SCPN labeling (Ctb) at P3 and analysis at P6 in the somatosensory cortex.

(M) Quantification of SCPN (Ctb^+) labeled by BrdU at either E11.5, E12.5, E13.5, or E14.5 ($BrdU^+$ at E11.5-Ctb^+/Ctb^+: *Tle4*^{KO} vs. controls, 11% vs. 0%; $BrdU^+$ at E12.5-Ctb^+/Ctb^+: *Tle4*^{KO} vs. controls, 8% vs. 1%).

(N) BrdU and CTIP2 co-labeling ($BrdU^+$ at E12.5-$CTIP2^+$: *Tle4*^{KO} vs. control, 42% vs. 21%; $p < 0.01$).

(O–Q) BrdU and FOG2 co-labeling ($BrdU^+$ at E11.5-$FOG2^+$: *Tle4*^{KO} vs. control, 8% vs. 37%; $p < 0.01$; $BrdU^+$ at E12.5-$FOG2^+$: *Tle4*^{KO} vs. control, 10% vs. 28%); n = 5 for BrdU at E11.5, E12.5, and E13.5; n = 3 for BrdU at E14.5.

(R) Identification of dual-projecting LV-CThPN via FB (blue) injection in somatosensory thalamus and Ctb (red) injection in the pyramidal tract at P3. Analysis in somatosensory cortex at P8.

(S and T) In *Tle4*^{KO} and control mice, neurons with dual projections (FB^+-Ctb^+) are located only in LV (white arrowheads).

(U and V) Confocal images of squared areas in (S) and (T). (U′ and V′) LV-CThPN (FB^+-Ctb^+) in *Tle4*^{KO} and control mice. (U″ and V″) No fate-converted SCPN (Ctb^+ in LV_{ex} or LVI) in *Tle4*^{KO} mice are double labeled (open arrowheads).

(W) Quantification of SCPN, LV-CThPN, and LVI-CThPN in the somatosensory cortex; n = 5 mice per genotype.

(X) Schematic summary.

Statistics for all quantification, ANOVA-Tukey, *$p < 0.05$, **$p < 0.01$. Error bars, SEM. Scale bars, 250 μm (B and C); 100 μm (B′ and C′); 200 μm (E–I); 20 μm (K′, L′, O, U′, and V″); 100 μm (U and V).

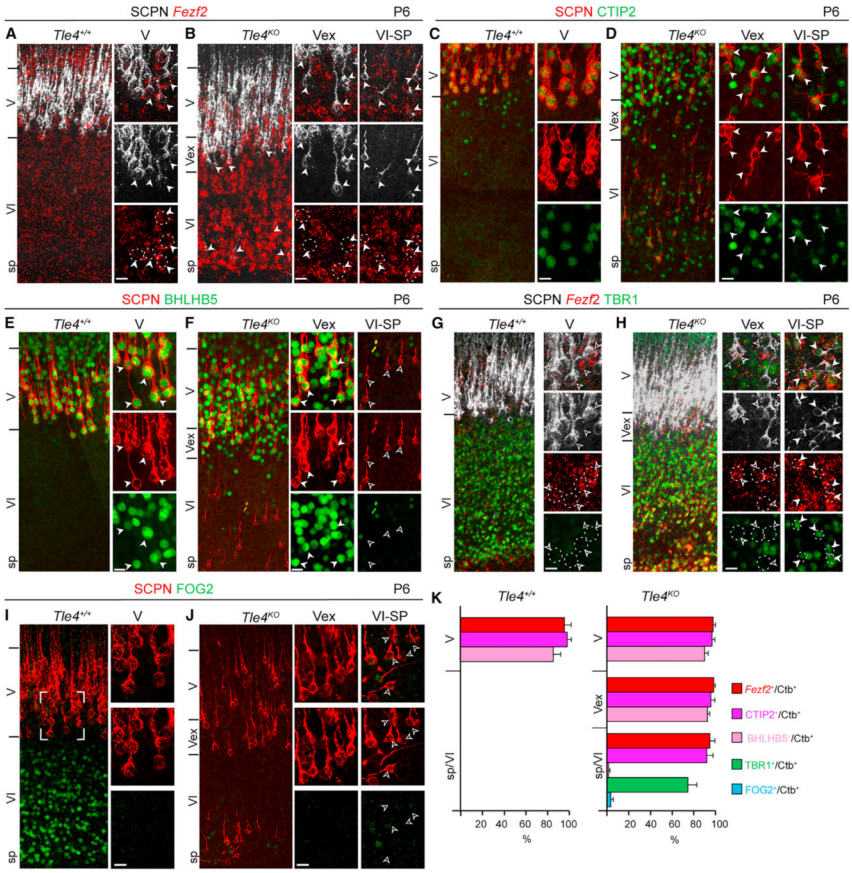

Figure 4. Expression of SCPN and CThPN molecular controls by fate-converted SCPN in *Tle4*^{KO} mice

(A and B) ISH for *Fezf2* (red) and SCPN labeling with Ctb (white). SCPN expressing *Fezf2* (white arrowheads).

(C and D) Co-localization of CTIP2 (green) and SCPN labeling with Ctb (red) (SCPN-CTIP2$^+$ in LV$_{ex}$, LVI-subplate in *Tle4*^{KO} mice, white arrowheads).

(E and F) Co-localization of BHLHB5 (green) and Ctb (red) in LV$_{ex}$-fate-converted SCPN in *Tle4*^{KO} mice (open arrowheads).

(G and H) TBR1 immunolabeling (green), *Fezf2* ISH (red), SCPN retrograde labeling with Ctb (white). Fate-converted SCPN in LV$_{ex}$ are *Fezf2*$^+$-TBR1$^-$ (open arrowheads). Fate-converted SCPN in LVI are *Fezf2*$^+$-TBR1$^+$ (solid arrowheads). Dashed lines encircle *Fezf2*$^+$ neuron somata.

(I and J) Co-localization of FOG2 (green) and SCPN labeling Ctb (red).

(K) Percentage of SCPN expressing *Fezf2*, CTIP2, BHLHB5, TBR1, or FOG2 in LV and LVI subplate in WT and in LV, LV$_{ex}$, and LVI subplate in *Tle4*^{KO} mice. SCPN labeling at P3 and analysis at P6. Quantification in somatosensory cortex, n = 5 per genotype. Error bars, SEM. Scale bars, 20 μm (A–J).

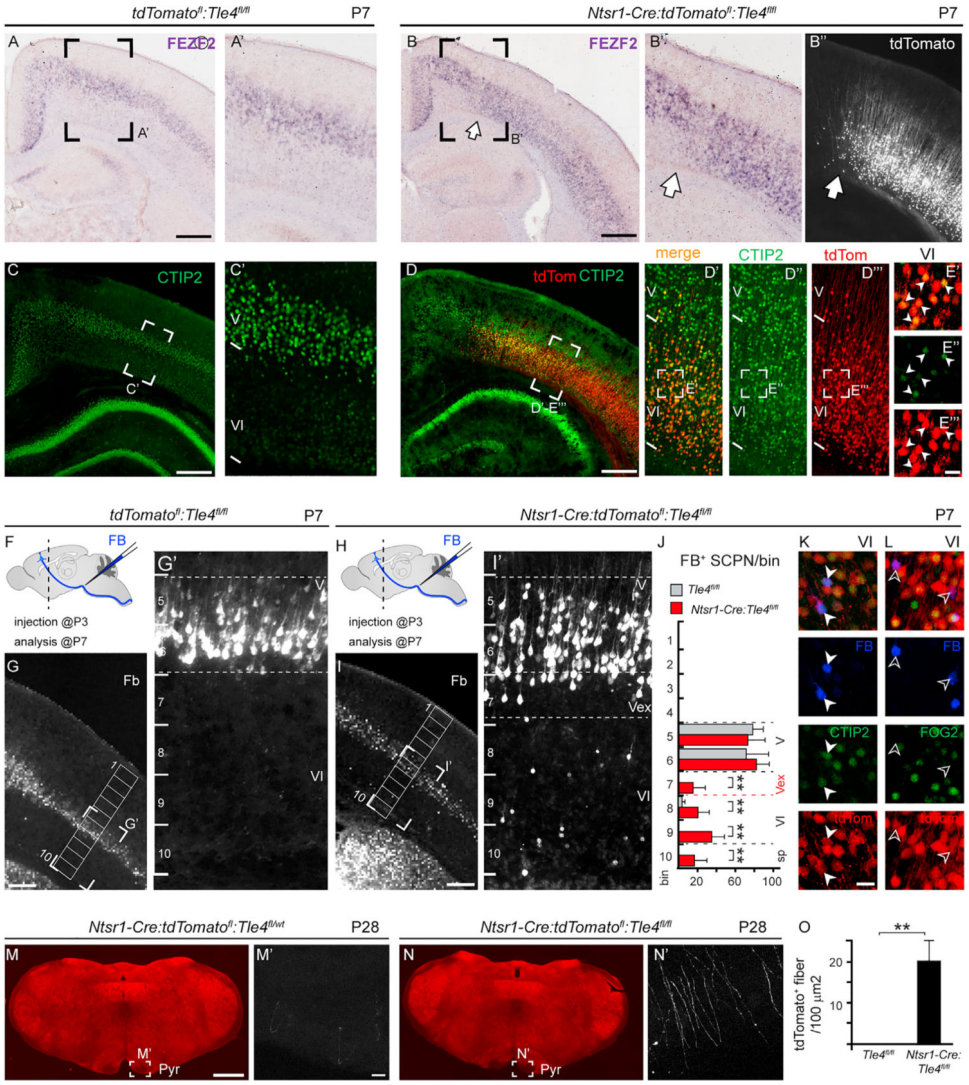

Figure 5. *Tle4* is required perinatally to maintain CThPN identity during thalamic innervation

(A–B′) *Fezf2* ISH and CTIP2 immunolabeling (C–E) in *Ntsr1-Cre:tdTomato^{fl}:Tle4$^{fl/fl}$* mice. (B′ and B″) Ntsr1-Cre expression limit between somatosensory and motor cortices (white arrow). Magnified insets from boxed areas in low-magnification images. (F and H) SCPN labeling approach by FB injection into pyramidal tract (P3). Analysis (P7) in somatosensory cortex.

(G–I) Presence of SCPN (FB$^+$) in LVI and LV$_{ex}$ in *Ntsr1-Cre:tdTomato^{fl}:Tle4$^{fl/fl}$* mutants, but not in *tdTomato^{fl}:Tle4$^{fl/fl}$* controls.

(J) Distribution of SCPN (FB$^+$) across cortical thickness; n = 4 mice per genotype. Mean FB$^+$ cells/bin ± SEM; ANOVA-Tukey, **p < 0.01.

(K and L) In *Ntsr1-Cre:tdTomato^{fl}:Tle4$^{fl/fl}$* mice, reprogrammed SCPN (tdTomato$^+$-FB$^+$ in LV$_{ex}$ and LVI) upregulate CTIP2 (solid arrowheads) and downregulate FOG2 (open arrowheads).

(M–O) Quantification of tdTomato$^+$ axons from Ntsr1-Cre-expressing neurons in pyramidal tract at P28 (n = 3 per genotype, unpaired t test, **p < 0.01). Error bars, SEM.

Scale bars, 500 μm (A–D); 250 μm (G and I); 20 μm (E′–E″′, K, L, and M′); 1 mm (M).

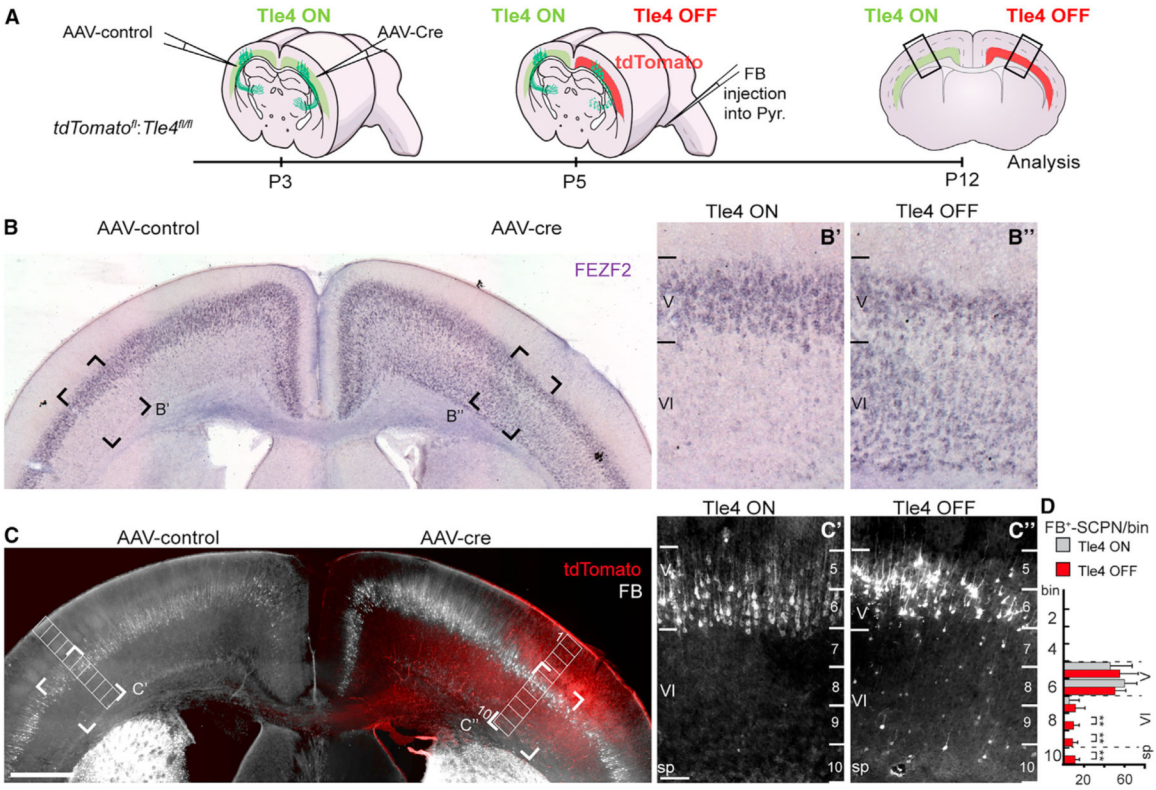

Figure 6. Differentiated CThPN transform their identity in the absence of *Tle4* function during post-natal maturation

(A) Experimental approach. *TdTomato*^{fl}:*Tle4*$^{fl/fl}$ mice are injected at P3 with AAV-Cre on one side of the cortex and AAV-control on the contralateral side. At the time of AAV-injections, *Tle4* is expressed in both hemispheres (*Tle4* ON). At P5, FB is injected into the pyramidal tract (Pyr). At this point, *Tle4* is not expressed in the area injected with AAV-Cre (*Tle4* OFF). Analysis at P12 in somatosensory cortex.

(B) *Fezf2* ISH demonstrates upregulation in LVI of the AAV-Cre-injected area (tdTomato^{+} in C), but not on the contralateral side (B′ and B″).

(C) Presence of FB^{+} neurons in LVI (post-natally reprogrammed-SCPN) in AAV-Cre-injected area. (C′ and C″) Magnified insets showing retrograde labeling in somatosensory cortex (grids in C).

(D) Quantification of SCPN across cortical thickness (n = 6, mean FB^{+} cells/bin ± SEM; ANOVA-Tukey, **p < 0.01).

Error bars, SEM. Scale bars, 500 μm (C); 100 μm (C′).

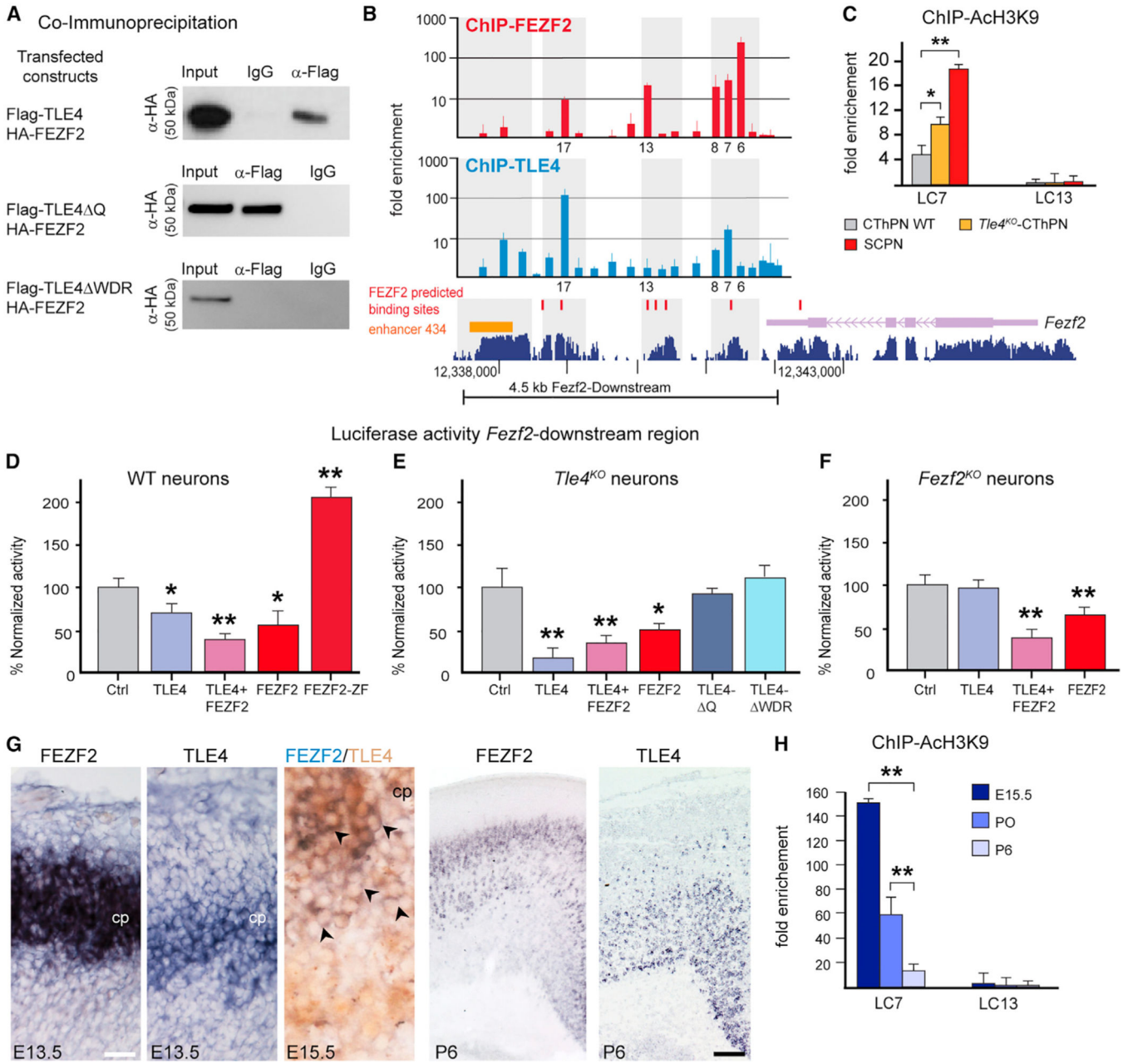

Figure 7. TLE4 and FEZF2 form a complex that controls *Fezf2* expression level in developing and maturing CThPN

(A) CoIP of FLAG-TLE4 and HA-FEZF2 from E15.5 cortical neurons. Pull-downs with full-length TLE4 (FLAG-TLE4), FLAG-TLE4ΔQ, or FLAG-TLE4ΔWDR. Anti-FLAG antibody or non-specific IgG used for pull-downs and anti-HA for immunoblots.

(B) ChIP-qPCR reveals binding of FEZF2 and TLE4 in the 4.5-kb region downstream of *Fezf2*. Amplified loci numbered from 1 (at *Fezf2* 3′ UTR) to 23 (at 4.5 kb downstream of *Fezf2*). Predicted *Fezf2* binding sites (red marks, lower map), enhancer 434 (orange bar, lower map), and *Fezf2* gene sequence (purple, lower map) are shown for reference.

ChIP-FEZF2 and ChIP-TLE4 expressed as fold-enrichment normalized to control ChIP-IgG for each amplicon. Error bars represent SEM from four replicates.

(C) ChIP-AcH3K9 qPCR analysis for LC7 and LC13 normalized to *Gapdh* (n = 4 replicates per group; ANOVA-Tukey, *p < 0.05, **p < 0.01).

(D–F) Luciferase activity relative to control (ctrl; pGL3-*Fezf2-downstream*-Luciferase alone) in the presence of TLE4, TLE4+FEZF2, FEZF2, and FEZF2-ZF in cortical neurons from E15.5 WT embryos (D); in the presence of TLE4, TLE4+FEZF2, FEZF2, TLE4ΔQ, and TLE4ΔWDR in neurons from E15.5 $Tle4^{KO}$ embryos (E); and in the presence of TLE4, TLE4+FEZF2, and FEZF2 in neurons from E15.5 $Fezf2^{KO}$ embryos (F). Seven replicates per condition for experiments with WT and $Tle4^{KO}$ neurons and five replicates per condition for experiments with $Fezf2^{KO}$ neurons (ANOVA-Tukey, *p < 0.05, **p < 0.01).

(G) ISH for *Fezf2* and *Tle4* in adjacent 10-μm sections at E13.5. *Fezf2* ISH and TLE4 immunolabeling at E15.5 demonstrate co-localization (black arrowheads). *Fezf2* and *Tle4* ISH at P6.

(H) ChIP-AcH3K9 in LC7 and LC13 at E15.5, P0, and P6 normalized to *Gapdh*. Four replicates per group; ANOVA-Tukey, *p < 0.05; **p < 0.01. Error bars, SEM. Scale bars, 20 μm (G, E13.5); 100 μm (G, P6).

KEY RESOURCES TABLE

REAGENT or RESOURCE	SOURCE	IDENTIFIER
Antibodies		
rat anti-BrdU	Accurate Chemical and Scientific Corporation	RRID:AB_2341179
rat anti-CTIP2	Abcam	Cat# ab28448, RRID:AB_1140055
rabbit anti-DARPP-32	Cell Signaling Technology	Cat# 2306S, RRID:AB_823479
rabbit anti-FOG2	Santa Cruz	Cat# sc-10755, RRID:AB_2218978
goat anti-NURR1	R&D Systems	Cat# AF2156, RRID:AB_2153894
rabbit anti-TBR1	Abcam	Cat# ab31940, RRID:AB_2200219
rabbit anti-FOXP2	Abcam	Cat# ab1307, RRID:AB_1268914
rabbit anti-TLE4	Santa Cruz	Cat# sc-9125, RRID:AB_793141
Rabbit anti-HA	Covance	Cat# MMS-101R, RRID:AB_291262
Anti-AcH3K9	Millipore	Cat #17–658, RRID:AB_1587124
Anti-Flag	Sigma	Cat # F7425; RRIB:AB_439687
Bacterial and virus strains		
AAV 2/1 CAG-CRE	Vector core at Massachusetts General Hospital, Boston, MA; Maguire et al., 2013[58]	N/A
AAV 2/1 CAG	Vector core at Massachusetts General Hospital, Boston, MA; Maguire et al., 2013[58]	N/A
Chemicals, peptides, and recombinant proteins		
Cholera Toxin B subunit,	ThermoFisher	Cat # C34776
Fast Blue	Polysciences	Cat # 17740–1
Critical commercial assays		
LightCycler Fast start DNA Master SYBER Green I	Roche	Cat # 3515885001
Dual-Glo system	Promega	Cat# E2940
Deposited data		
N/A		
Experimental models: Organisms/strains		
Tle4^{KO} mice	Wheat et al., 2014[13]	N/A
Tle4^{floxed} mice	Wheat et al., 2014[13]	N/A
Emx1-Cre mice	Jacklson Labs	stock # 005628
Ai14	Jacklson Labs	stock # 007914
Ntsr1-Cre	GENSAT, MMRRC	stock # 030648-UCD
Rbp4-Cre	GENSAT, MMRRC	stock # 031125-UCD
Fezf2-PLAP	Chen at al., 2005a[31]	N/A
Recombinant DNA		

REAGENT or RESOURCE	SOURCE	IDENTIFIER
pCAG-HA-Fezf2	This paper	N/A
pCAG-Flag-Tle4	This paper	N/A
pCAG-Flag-Tle4ΔQ	This paper	N/A
pCAG-Flag-Tle4ΔWDR	This paper	N/A
pGL3-luc;	Promega	Cat #E1751
pGL3-*Fezf2*-downstram-luc	This paper	N/A
Software and algorithms		
Prism	GraphPad	RRID:SCR_002798
Fiji ImageJ	Image J-NIH	RRID:SCR_002285